

Non-standard signatures of vector-like quarks in a leptophobic 221 model.

Kasinath Das,^{*} Tanmoy Mondal,[†] and Santosh Kumar Rai[‡]

Regional Centre for Accelerator-based Particle Physics,

Harish-Chandra Research Institute, HBNI,

Chhatnag Road, Jhusi, Allahabad 211019, India

(Dated: November 17, 2021)

Abstract

We consider vector-like quarks in a leptophobic 221 model characterized by the gauge group $SU(2)_L \times SU(2)_2 \times U(1)_X$, where the $SU(2)_2$ is leptophobic in nature. We discuss about the pattern of mixing between Standard Model quarks and vector-like quarks and how we prevent tree level flavour-changing interactions in the model. The model also predicts tauphilic scalars decaying mostly to tau leptons. We consider a typical signal of the model in the form of pair production of top-type vector-like quarks which decays to the tauphilic scalars and a third generation quark. We analyze the resulting final state signal for the 13 TeV LHC, containing $\geq 3j(1b) + \geq 2\tau + \geq 1l$ and discuss the discovery prospects of such vector-like quarks with non-standard decay modes.

Keywords: Extended Gauge Models, Vector-like Quarks, Flavour Changing Neutral Currents

^{*} kasinath.das91@gmail.res.in

[†] tanmoymondal@hri.res.in

[‡] skrai@hri.res.in

I. INTRODUCTION

As the Large Hadron Collider (LHC) churns out more and more data and gets ready for an energy upgrade, lack of new physics signal at the high energy frontier only makes us more intrigued with what picture of beyond Standard Model (SM) could eventually emerge. The SM itself highlights the great success of gauge theory and a natural extension would be in the form of additional gauge symmetries with new matter fields. We know that all the three generations of matter fields in the SM are chiral in nature. The possibility of a fourth generation of chiral fermions, especially quarks has been excluded by the Higgs signal strength measurements along with the electroweak precision data [1]. However the possibility of having vector-like quarks (VLQ) whose left- and right-chiral components transform in the same way under the SM gauge group still exists and are being searched for at the LHC.

The collider signatures of a VLQ depends on its possible decay modes. The existing searches for VLQs are under the assumption that they decay to a SM boson and a SM quark. For example searches on top-like VLQ with electric charge $Q = +\frac{2}{3}$ assume that it decays to Zt , W^+b and ht and for a bottom-like VLQ with electric charge $Q = -\frac{1}{3}$, the decay modes are Zb , W^-t and hb . Assuming strong pair production, both ATLAS and CMS collaborations have obtained different lower limits on the masses of third generation VLQs for different branching ratio hypotheses [2–7]. The most stringent lower bound on the mass of a top-like VLQ obtained by using the LHC Run 2 data is 1.3 TeV given by CMS [2] and 1.43 TeV given by ATLAS [6] while the most stringent lower bound on the mass of a bottom-like VLQ is 1.24 TeV given by CMS [2] and 1.35 TeV given by ATLAS [5]. Since the single production of VLQs depend on the mixing between VLQs and SM quarks, based on the searches for single-production of VLQs both CMS and ATLAS collaborations have given exclusion limits for the product of production cross section and branching fraction for different mass values [8–10]. Extensive phenomenological studies on VLQs in standard decay scenarios exist in literature [11–17].

Exotic fermions are a necessary ingredient in some gauge extended models for anomaly cancellation, e.g., exotic quarks in leptophobic 221 model [18, 19], exotic leptons in hadrophobic 221 model [18] and exotic fermions in almost all $U(1)'$ extensions [20]. These exotic fermions become vector-like once the full symmetry group breaks down to the SM gauge group. These fermions are quasi-chiral in nature, i.e., they are vector-like under the SM gauge group but chiral under the extra gauge group [20].

VLQs in gauge extended models can have interesting collider signatures because the rich spectrum of the model opens up non-standard decay modes for the VLQs. In this work we have considered the collider signatures of certain non-standard decay modes of top-like VLQ in a leptophobic 221 model characterized by the gauge group $SU(2)_1 \times SU(2)_2 \times U(1)_X$.

Because of the presence of the non-standard decay modes the existing constraints on the masses of VLQs will get significantly relaxed and the VLQ can lie at the sub-TeV scale. Phenomenological studies of VLQs having non-standard decay modes exist in literature for various non-minimal extensions of SM [21–34]. Collider signatures of vector-like quarks in $U(1)$ gauge extensions have been considered in [35–37].

In general, the mixing between SM quarks and VLQs which play an important role in the phenomenology of VLQs also generate tree level flavour-changing neutral current (FCNC) interactions of SM quarks with the Z boson. Several studies on the mixing of VLQs with SM quarks are available in the literature [16, 38–43] which take into account constraints from flavour physics and electroweak precision measurements. Mixings are strongly constrained from FCNC processes. Even in the presence of mixings with VLQs the possibility of avoiding tree level FCNC interactions is possible for judiciously chosen mixing patterns [44]. We discuss such a mixing pattern for the leptophobic 221 model which avoids tree level flavour-changing interactions with the Z and Z' . For general mixing scenarios between VLQs and SM quarks, all the neutral scalars present in the model have flavour-changing interactions, thus making it difficult to get a 125 GeV neutral Higgs and simultaneously satisfying constraints from FCNC processes. We show that it is possible to avoid flavour-changing interactions for certain neutral scalars (non-FCNH scalars), which can then lie at sub-TeV scale. In this work we study the collider signatures of the third generation top-type VLQ decaying to a final state with one of these non-FCNH scalars (other than the 125 GeV Higgs) and a third generation SM quark and the scalars then decay dominantly to tau leptons.

The paper is organized as follows. In Section II we discuss our model. In Section III we discuss about the interaction of the VLQs with the SM gauge bosons. In Section IV we discuss the pattern of mixing between the SM quarks and the VLQs for which FCNC interactions of SM quarks with Z -boson and the FCNH interactions with the SM-Higgs boson is zero at the tree level. In Section V we discuss the possible phenomenology of VLQs in the model and explore the possible collider signatures in Section VI. Finally we conclude and summarize in Section VII.

II. THE MODEL

The $SU(2)$ extensions of the SM characterized by the gauge group $SU(3)_C \times SU(2)_1 \times SU(2)_2 \times U(1)_X$ are generally called 221 models in the literature. Depending on the way the SM fermions transform under the gauge groups, different versions of 221 models are possible, *viz.* leptophobic, hadrophobic and left-right symmetric etc. The model is called leptophobic when the SM right-chiral leptons are singlets under $SU(2)_2$, hadrophobic when the right-chiral SM quarks are singlets under $SU(2)_2$ and left-right symmetric when both

the SM right-chiral quarks and the right-chiral leptons (with the addition of right-chiral neutrinos to the model) form doublets under $SU(2)_2$. The most popular among all 221 models is the left-right symmetric model [45–50]. A general classification of all 221 models has been done in [18] based on two types of symmetry breaking patterns of the gauge group. The two patterns are as follows :

- Type-I : $SU(2)_1$ is identified with $SU(2)_L$ of SM. The first stage of symmetry breaking is $SU(2)_2 \times U(1)_X \rightarrow U(1)_Y$. The second stage of symmetry breaking is $SU(2)_L \times U(1)_Y \rightarrow U(1)_{em}$.
- Type-II : $U(1)_X$ is identified with $U(1)_Y$ of SM. The first stage of symmetry breaking is $SU(2)_1 \times SU(2)_2 \rightarrow SU(2)_L$. The second stage of symmetry breaking is $SU(2)_L \times U(1)_Y \rightarrow U(1)_{em}$.

Certain type of 221 models need exotic fermions for the cancellation of anomalies. For example, the leptophobic 221 model needs exotic quarks and the hadrophobic 221 model requires exotic leptons. These exotic fermions become vector-like after the breaking of the full symmetry group down to SM gauge group.

In this work we consider the leptophobic 221 model, which follows the type-I symmetry breaking pattern described above and the SM leptons are singlets under the $SU(2)_2$ gauge group¹. We will denote $SU(2)_1$ as $SU(2)_L$ throughout the article. The scalar sector of the model contains two scalar doublets represented by H_1 and H_2 , and a bi-doublet scalar represented by Φ . The symmetry breaking of the full gauge group to $U(1)_{em}$ by the scalars occurs in two stages :

$$\begin{aligned} \text{Stage I : } & SU(2)_2 \times U(1)_X \xrightarrow{\langle H_2 \rangle} U(1)_Y, \\ \text{Stage II : } & SU(2)_L \times U(1)_Y \xrightarrow{\langle \Phi \rangle, \langle H_1 \rangle} U(1)_{em}. \end{aligned} \quad (1)$$

The first stage of symmetry breaking of the full gauge group to the SM gauge group ($SU(2)_L \times U(1)_Y$) is achieved by the vacuum expectation value (VEV) of H_2 , which is a doublet under $SU(2)_2$. The subsequent second stage breaking of the SM gauge group to the $U(1)_{em}$ gauge group occurs, once Φ , a bi-doublet under $SU(2)_L \times SU(2)_2$ or H_1 , a doublet under $SU(2)_L$ obtains a VEV. The fermion and scalar field content of the model and their corresponding charges under the symmetry group are listed in Table. 1. The left chiral fields Q_{iL} and L_{iL} transform as doublets under $SU(2)_L$ and are identical to the left chiral fields of the SM transforming under the $SU(2)_L$. The right handed quarks (u_{iR}^0, d_{iR}^0)

¹ The model has been considered previously in [19] to explain the reported excess for a narrow width resonance around 2 TeV in the WZ , WW , and ZZ channel by the ATLAS collaboration [51] using the 20.3 fb⁻¹ of data of 8 TeV LHC.

$Q_{iL} = \begin{pmatrix} u_{iL}^0 \\ d_{iL}^0 \end{pmatrix}$	$(3, 2, 1, \frac{1}{6})$	$Q_{iR} = \begin{pmatrix} u_{iR}^0 \\ d_{iR}^0 \end{pmatrix}$	$(3, 1, 2, \frac{1}{6})$
$XQ_{iL} = \begin{pmatrix} xu_{iL}^0 \\ xd_{iL}^0 \end{pmatrix}$	$(3, 1, 2, \frac{1}{6})$	xu_{iR}^0 xd_{iR}^0	$(3, 1, 1, \frac{2}{3})$ $(3, 1, 1, -\frac{1}{3})$
$L_{iL} = \begin{pmatrix} \nu_L \\ e_{iL} \end{pmatrix}$	$(1, 2, 1, -\frac{1}{2})$	e_{iR}	$(1, 1, 1, -1)$
Φ	$(1, 2, 2, 0)$	H_1 H_2	$(1, 2, 1, -\frac{1}{2})$ $(1, 1, 2, -\frac{1}{2})$

TABLE 1: Fields and their corresponding charges under the gauge group $SU(3)_C \times SU(2)_1 \times SU(2)_2 \times U(1)_X$. The model contains three generations of fermions for $i = 1, 2, 3$.

form doublets under the gauge group $SU(2)_2$ as it is in case of left-right symmetric model. But unlike the left-right symmetric model for this version of a 221 model there are no lepton doublets under the $SU(2)_2$ gauge group and hence the $SU(2)_2$ is leptophobic in nature. Therefore the model contains exotic quarks to ensure triangle anomaly cancellation. Each generation of the exotic quark sector of the model contains a field XQ_{iL} formed out of two left chiral fields xu_{iL}^0 and xd_{iL}^0 , and transforms as a doublet under the $SU(2)_2$ gauge group. For each generation the model also contains two right chiral fields xu_{iR}^0 and xd_{iR}^0 which are singlets under both $SU(2)_L$ and $SU(2)_2$. The right handed leptons e_{iR} transform as singlets under both the $SU(2)$ gauge groups.

Note that the exotic quarks present in the model are chiral in nature under the full unbroken gauge group. However, after the stage-I symmetry breaking $SU(2)_2 \times U(1)_X \rightarrow U(1)_Y$, the exotic quarks become vector-like under the $SU(2)_L \times U(1)_Y$, which is the SM gauge group. This feature can be realized by following the definition of hypercharge quantum number Y after the first stage of symmetry breaking which is given by

$$Y = T_{23} + Q_X, \quad (2)$$

where T_{23} denote the diagonal generator of $SU(2)_2$ and Q_X represents the charge for the gauge group $U(1)_X$. The hypercharge quantum number for the exotic quarks are given by $Y(xu_L^0) = \frac{2}{3} = Y(xu_R^0)$ and $Y(xd_L^0) = -\frac{1}{3} = Y(xd_R^0)$, i.e. they are vector-like with respect to the $SU(2)_L \times U(1)_Y$ gauge group.

After the stage II of symmetry breaking, the electric charge for a field is given by

$$Q = T_{13} + Y, \quad (3)$$

where T_{13} denote the diagonal generator of $SU(2)_1$. Following the above definition the electric charges for the VLQs are given by $Q(xu_i^0) = +\frac{2}{3}$ and $Q(xd_i^0) = -\frac{1}{3}$.

A. Yukawa Sector

The Yukawa Lagrangian including the bilinear mass terms for the model is given by

$$\begin{aligned} -L_{Yukawa} = & Y_{ij}^q \overline{Q}_{iL} \Phi Q_{jR} + Y_{ij}^{qC} \overline{Q}_{iL} \widetilde{\Phi} Q_{jR} + Y_{ij}^{xqxu} \overline{XQ}_{iL} xu_{jR}^0 H_2 \\ & - Y_{ij}^{xqxd} \overline{XQ}_{iL} xd_{jR}^0 \widetilde{H}_2 + Y_{ij}^{qxu} \overline{Q}_{iL} xu_{jR}^0 H_1 - Y_{ij}^{qxd} \overline{Q}_{iL} xd_{jR}^0 \widetilde{H}_1 \\ & + \mu_{ij} \overline{XQ}_{iL} Q_{jR} + Y_{ij}^L \overline{L}_{iL} e_{jR} \widetilde{H}_1 + H.C., \end{aligned} \quad (4)$$

where $i, j = 1, 2, 3$ and we define the fields,

$$\widetilde{\Phi} = \sigma_2 \Phi^* \sigma_2 \equiv (1, 2, 2, 0), \quad \widetilde{H}_1 = i\sigma_2 H_1^* \equiv (1, 2, 1, \frac{1}{2}), \quad \widetilde{H}_2 = i\sigma_2 H_2^* \equiv (1, 1, 2, \frac{1}{2}). \quad (5)$$

The Y matrices in the above Lagrangian are Yukawa couplings. Note that after the scalars get VEVs the Y_{ij}^q and Y_{ij}^{qC} terms will give masses to the SM quarks while the Y_{ij}^{xqxu} and Y_{ij}^{xqxd} terms give masses to the VLQs. The terms in the Lagrangian containing Y_{ij}^{qxu} , Y_{ij}^{qxd} and the bilinear term with μ_{ij} will generate mixing between the SM quarks and the VLQs. Since the model does not contain any lepton doublet under $SU(2)_2$ gauge group, the charged leptons will get mass from the VEV of the doublet H_1 unlike the quarks which get their mass from the bi-doublet Φ .

B. Scalar Sector

The tree level scalar potential for the model in terms of a complete set of linearly independent gauge invariant terms is given by

$$\begin{aligned} V = & -\mu_1^2 \text{Tr}[\Phi^\dagger \Phi] - \left\{ \mu_2^2 \text{Tr}[\widetilde{\Phi}^\dagger \Phi] + \mu_2^{*2} \text{Tr}[\Phi^\dagger \widetilde{\Phi}] \right\} - \mu_3^2 H_1^\dagger H_1 - \mu_4^2 H_2^\dagger H_2 \\ & + \left\{ M_1 H_1^\dagger \Phi H_2 + M_1^* H_2^\dagger \Phi^\dagger H_1 \right\} + \left\{ M_2 H_1^\dagger \widetilde{\Phi} H_2 + M_2^* H_2^\dagger \widetilde{\Phi}^\dagger H_1 \right\} \\ & + \lambda_1 \left\{ \text{Tr}[\Phi^\dagger \Phi] \right\}^2 + \left\{ \lambda_2 \{ \text{Tr}[\Phi^\dagger \widetilde{\Phi}] \}^2 + \lambda_2^* \{ \text{Tr}[\widetilde{\Phi}^\dagger \Phi] \}^2 \right\} + \lambda_3 \text{Tr}[\Phi^\dagger \widetilde{\Phi}] \text{Tr}[\widetilde{\Phi}^\dagger \Phi] \\ & + \left\{ \lambda_4 \text{Tr}[\Phi^\dagger \Phi] \text{Tr}[\Phi^\dagger \widetilde{\Phi}] + \lambda_4^* \text{Tr}[\Phi^\dagger \Phi] \text{Tr}[\widetilde{\Phi}^\dagger \Phi] \right\} + \beta_1 \text{Tr}[\Phi^\dagger \Phi] (H_1^\dagger H_1) \\ & + \left\{ \beta_2 \text{Tr}[\widetilde{\Phi}^\dagger \Phi] (H_1^\dagger H_1) + \beta_2^* \text{Tr}[\Phi^\dagger \widetilde{\Phi}] (H_1^\dagger H_1) \right\} + \beta_3 \widetilde{H}_1^\dagger \Phi \Phi^\dagger \widetilde{H}_1 \\ & + \alpha_1 \text{Tr}[\Phi^\dagger \Phi] (H_2^\dagger H_2) + \left\{ \alpha_2 \text{Tr}[\widetilde{\Phi}^\dagger \Phi] (H_2^\dagger H_2) + \alpha_2^* \text{Tr}[\Phi^\dagger \widetilde{\Phi}] (H_2^\dagger H_2) \right\} \\ & + \alpha_3 \widetilde{H}_2^\dagger \Phi^\dagger \Phi \widetilde{H}_2 + \rho_1 (H_1^\dagger H_1)^2 + \rho_2 (H_2^\dagger H_2)^2 + \rho_3 (H_1^\dagger H_1) (H_2^\dagger H_2). \end{aligned} \quad (6)$$

In general the parameters from the set $\{\mu_1^2, \mu_3^2, \mu_4^2, \lambda_1, \lambda_3, \beta_1, \beta_3, \alpha_1, \alpha_3, \rho_1, \rho_2, \rho_3\}$ are real and others are complex. In this paper, for simplicity we have considered all the parameters to be real.

The scalar fields in component form can be written as

$$H_1 = \begin{pmatrix} \chi^0 \\ \chi^- \end{pmatrix}, \quad H_2 = \begin{pmatrix} \chi'^0 \\ \chi'^- \end{pmatrix}, \quad \Phi = \begin{pmatrix} \phi_1^0 & \phi_1^+ \\ \phi_2^- & \phi_2^0 \end{pmatrix}, \quad (7)$$

where

$$\begin{aligned} \phi_1^0 &= \frac{1}{\sqrt{2}}(v_1 + \phi_1^{0r} + i\phi_1^{0i}), & \phi_2^0 &= \frac{1}{\sqrt{2}}(v_2 + \phi_2^{0r} + i\phi_2^{0i}), \\ \chi^0 &= \frac{1}{\sqrt{2}}(v_3 + \chi^{0r} + i\chi^{0i}), & \chi'^0 &= \frac{1}{\sqrt{2}}(u + \chi'^{0r} + i\chi'^{0i}). \end{aligned} \quad (8)$$

The structure of VEVs for the scalar fields are

$$\langle H_1 \rangle = \frac{1}{\sqrt{2}} \begin{pmatrix} v_3 \\ 0 \end{pmatrix}, \quad \langle H_2 \rangle = \frac{1}{\sqrt{2}} \begin{pmatrix} u \\ 0 \end{pmatrix}, \quad \langle \Phi \rangle = \frac{1}{\sqrt{2}} \begin{pmatrix} v_1 & 0 \\ 0 & v_2 \end{pmatrix}. \quad (9)$$

The set of tadpole equations $\{\frac{\partial V}{\partial \phi_1^{0r}} = 0, \frac{\partial V}{\partial \phi_2^{0r}} = 0, \frac{\partial V}{\partial \chi^{0r}} = 0, \frac{\partial V}{\partial \chi'^{0r}} = 0\}$ have been solved in terms of $\mu_1^2, \mu_2^2, \mu_3^2, \mu_4^2$ and are given in the appendix A. The components of the mass square matrices for the CP even scalars (M_S^2) in the $(\phi_1^{0r}, \phi_2^{0r}, \chi^{0r}, \chi'^{0r})$ basis, for the CP odd scalars (M_P^2) in the $(\phi_1^{0i}, \phi_2^{0i}, \chi^{0i}, \chi'^{0i})$ basis and for the charged scalars (M_C^2) in the $(\phi_1^+, \phi_2^+, \chi'^+, \chi^+)$ basis are given in appendix B 1, B 2 and B 3 respectively.

There are four physical CP even scalars in the model. Two of the four CP odd scalars will be physical and the other two are massless Goldstone bosons which become part of the two massive neutral gauge bosons. Similarly there will be two physical charged scalars and the other two Goldstone bosons become part of the two massive charged gauge bosons. Hence, after the spontaneous symmetry breaking followed by the Higgs mechanism, the physical spectrum of the scalar sector consists of four neutral CP even scalars, two neutral CP odd scalars and two charged scalars (and their antiparticles).

C. Gauge Boson Sector

The gauge couplings corresponding to the gauge groups $SU(2)_L$, $SU(2)_2$ and $U(1)_X$ are respectively represented by g_1 , g_2 and g_X . Based on the two stages of symmetry breaking pattern we define two mixing angles ϕ and θ_W in terms of which the gauge couplings are given by

$$g_1 = \frac{e}{\sin \theta_W}, \quad g_2 = \frac{e}{\cos \theta_W \sin \phi}, \quad g_X = \frac{e}{\cos \theta_W \cos \phi}. \quad (10)$$

After the stage I of symmetry breaking $SU(2)_2 \times U(1)_X \rightarrow U(1)_Y$ the gauge group becomes the Standard Model gauge group $SU(2)_L \times U(1)_Y$. The SM hypercharge gauge coupling g_Y for the gauge group $U(1)_Y$ is given by the relation $\frac{1}{g_Y^2} = \frac{1}{g_2^2} + \frac{1}{g_X^2}$. With the stage II of symmetry breaking $SU(2)_1 \times U(1)_Y \rightarrow U(1)_{em}$ the electromagnetic gauge coupling constant e is defined by $\frac{1}{e^2} = \frac{1}{g_1^2} + \frac{1}{g_Y^2}$. Here the angle θ_W denotes the weak mixing angle in the SM. At the end of the two stages of symmetry breaking the electromagnetic charge for any field in the model is defined by $Q = T_{13} + T_{23} + Q_X$.

The gauge bosons corresponding to the gauge groups are denoted by :

$$\begin{aligned} SU(2)_1 &: W_{1,\mu}^\pm, W_{1,\mu}^3; \\ SU(2)_2 &: W_{2,\mu}^\pm, W_{2,\mu}^3; \\ U(1)_X &: X_\mu. \end{aligned} \quad (11)$$

The mass square matrix for the charged gauge boson sector in the $(W_{1,\mu}^\pm, W_{2,\mu}^\pm)$ basis is given by

$$M_{W_1-W_2}^2 = \frac{1}{4} \begin{pmatrix} g_1^2(v_1^2 + v_2^2 + v_3^2) & -2g_1g_2v_1v_2 \\ -2g_1g_2v_1v_2 & g_2^2(u^2 + v_1^2 + v_2^2) \end{pmatrix}. \quad (12)$$

Since the vacuum expectation value v_3 gives masses to the charged leptons, for simplicity we consider the situation where $v_1^2 + v_2^2 \gg v_3^2$ and to have the stage II breaking at a higher scale we consider $u \gg v_1, v_2, v_3$. Based on this we define a small parameter ϵ which is given by $\frac{v^2}{u^2}$, where $v = \sqrt{v_1^2 + v_2^2 + v_3^2} \simeq 246$ GeV.

The mass eigenstates for the charged gauge boson sector in terms of the gauge eigenstates are given by

$$\begin{pmatrix} W^\pm \\ W'^\pm \end{pmatrix} = \begin{pmatrix} \cos \theta_{ww'} & \sin \theta_{ww'} \\ -\sin \theta_{ww'} & \cos \theta_{ww'} \end{pmatrix} \begin{pmatrix} W_1^\pm \\ W_2^\pm \end{pmatrix}, \quad (13)$$

with the mixing angle given up to order ϵ by the relation

$$\cos \theta_{ww'} \simeq 1 \quad \text{and} \quad \sin \theta_{ww'} \simeq \epsilon \frac{\sin \phi \sin 2\beta}{\tan \theta_W}, \quad \text{with} \quad \beta = \tan^{-1} \left(\frac{v_1}{v_2} \right). \quad (14)$$

The mass eigenstate W denotes the observed SM W boson while the new W' is heavy with mass at TeV scale. The mass squared matrix for the neutral gauge boson sector in the basis (W_1^3, W_2^3, X) is

$$\frac{1}{4} \begin{pmatrix} g_1^2(v_1^2 + v_2^2 + v_3^2) & -g_1g_2(v_1^2 + v_2^2) & -g_1g_Xv_3^2 \\ -g_1g_2(v_1^2 + v_2^2) & g_2^2(v_1^2 + v_2^2 + u^2) & -g_2g_Xu^2 \\ -g_1g_Xv_3^2 & -g_2g_Xu^2 & g_X^2(u^2 + v_3^2) \end{pmatrix}, \quad (15)$$

and the mass eigenstates are given by

$$\begin{pmatrix} Z' \\ Z \\ A \end{pmatrix} = \begin{pmatrix} \cos \theta_{zz'} & -\sin \theta_{zz'} & 0 \\ \sin \theta_{zz'} & \cos \theta_{zz'} & 0 \\ 0 & 0 & 1 \end{pmatrix} \begin{pmatrix} 1 & 0 & 0 \\ 0 & \cos \theta_W & -\sin \theta_W \\ 0 & \sin \theta_W & \cos \theta_W \end{pmatrix} \begin{pmatrix} \cos \phi & 0 & -\sin \phi \\ 0 & 1 & 0 \\ \sin \phi & 0 & \cos \phi \end{pmatrix} \begin{pmatrix} W_2^3 \\ W_1^3 \\ X \end{pmatrix}. \quad (16)$$

Among the mass eigenstates, A denotes massless photon, Z denotes the observed neutral heavy SM weak gauge boson and Z' , the heavier neutral gauge boson that has mass at TeV scale. Up to order ϵ the $Z - Z'$ mixing angle is given by

$$\cos \theta_{zz'} \simeq 1 \quad \text{and} \quad \sin \theta_{zz'} \simeq \epsilon \frac{\sin \phi \cos^3 \phi}{\sin \theta_W}. \quad (17)$$

III. INTERACTIONS OF VECTOR LIKE QUARKS WITH GAUGE BOSONS

The covariant derivative for a field determines its nature of interaction with the gauge bosons. To observe the vector-like nature of the interaction of exotic quarks with the SM gauge bosons we write those terms from the covariant derivative which contains neutral gauge bosons and that is given by

$$\begin{aligned} & g_1 T_{13} W_{1\mu}^3 + g_2 T_{23} W_{2\mu}^3 + g_X Q_x X_\mu \\ &= e Q A_\mu + \frac{e}{\sin \theta_W \cos \theta_W} \left\{ (T_{13} - Q \sin^2 \theta_W) + \epsilon \cos^2 \phi ((T_{13} - Q) \sin^2 \phi + T_{23}) \right\} Z_\mu \\ &+ \frac{e}{\sin \theta_W \cos \theta_W} \left\{ ((T_{13} - Q) \sin^2 \phi + T_{23}) \frac{\sin \theta_W}{\sin \phi \cos \phi} + \epsilon (Q \sin^2 \theta_W - T_{13}) \frac{\sin \phi \cos^3 \phi}{\sin \theta_W} \right\} Z'_\mu. \end{aligned} \quad (18)$$

By observing the term with Z_μ from Eq. 18 we can conclude that the interaction strength of the left chiral fields $xu_i^0(xd_i^0)_L$ with Z boson differs from the interaction strength for the right chiral fields $xu_i^0(xd_i^0)_R$ by a term proportional to ϵ . This is because the left chiral and the right chiral fields do not have same T_{23} value. Hence the interactions of the BSM quarks with the Z boson are vector-like in the limit $\epsilon \rightarrow 0$. The origin of the ϵ term is due to the $Z - Z'$ mixing. Since we are interested in the situation where $u \gg v$ and hence $\epsilon = \frac{v^2}{u^2} \ll 1$, we have identified the BSM exotic quarks (xu_i^0 and xd_i^0) as VLQs throughout the article.

Since the exotic quarks are singlets under $SU(2)_L$ the interaction strength of the exotic quarks with the W boson will be very small for small values of $W - W'$ mixing angle.

IV. FCNC IN THE PRESENCE OF VECTOR LIKE QUARKS

In SM there is no flavour-changing neutral current (FCNC) interactions of quarks with the Z boson at the tree level because the quarks with same electric charge have universal

charge assignments under the SM gauge group. But in models with VLQs this scenario of having universal charges under the gauge group of the model having the same electric charge breaks down. Hence the mixing between the SM quarks and the VLQs can generate tree level FCNC interactions for the SM quarks.

In our model this mixing is generated by the terms proportional to Y_{ij}^{qxd} , Y_{ij}^{qxu} and μ_{ij} in the Yukawa Lagrangian in Eq. 4. For models with vector like quarks the possibility of restricting tree level FCNC interactions exists for special choice of mixing patterns between the quarks and VLQs[44]. It has been shown in [44] that if one linear combination of VLQs mix with only one SM quark mass eigenstate then there will be no Z -boson mediated FCNC interaction at tree level. This would imply that each VLQ will have a corresponding SM quark (mass eigenstate) with which it mixes. We use this formalism [44] and discuss the scenario in which the FCNC interactions vanish for our model.

The 6×6 dimensional mass matrices for the up-quark sector and for the down-quark sector are respectively given by

$$\mathcal{M}^u = \begin{pmatrix} M^u & Y^{qxu} \frac{v_3}{\sqrt{2}} \\ \mu & Y^{xqxu} \frac{u}{\sqrt{2}} \end{pmatrix} \quad \text{and} \quad \mathcal{M}^d = \begin{pmatrix} M^d & Y^{qxd} \frac{v_3}{\sqrt{2}} \\ \mu & Y^{xqxd} \frac{u}{\sqrt{2}} \end{pmatrix}. \quad (19)$$

The matrices Y^{qxu} , Y^{qxd} , Y^{xqxu} , μ are 3×3 dimensional whose components are formed out of the Yukawa couplings in Eq. 4. The 3×3 matrices M^u and M^d are given by

$$\begin{aligned} M^u_{ij} &= \frac{1}{\sqrt{2}} (Y_{ij}^q v_1 + Y_{ij}^{qC} v_2) \\ M^d_{ij} &= \frac{1}{\sqrt{2}} (Y_{ij}^q v_2 + Y_{ij}^{qC} v_1). \end{aligned} \quad (20)$$

The quark gauge eigenstates ($\hat{\mathcal{U}}_{L/R}$, $\hat{\mathcal{D}}_{L/R}$) and the mass eigenstates ($\mathcal{U}_{L/R}$, $\mathcal{D}_{L/R}$) are represented by

$$\begin{aligned} \hat{\mathcal{U}}_{L/R} &= \begin{pmatrix} U^0 & XU^0 \end{pmatrix}_{L/R}^T \equiv \begin{pmatrix} u^0 & c^0 & t^0 & xu_1^0 & xu_2^0 & xu_3^0 \end{pmatrix}_{L/R}^T \\ \hat{\mathcal{D}}_{L/R} &= \begin{pmatrix} D^0 & XD^0 \end{pmatrix}_{L/R}^T \equiv \begin{pmatrix} d^0 & s^0 & b^0 & xd_1^0 & xd_2^0 & xd_3^0 \end{pmatrix}_{L/R}^T \\ \mathcal{U}_{L/R} &= \begin{pmatrix} U & XU \end{pmatrix}_{L/R}^T \equiv \begin{pmatrix} u & c & t & xu_1 & xu_2 & xu_3 \end{pmatrix}_{L/R}^T \\ \mathcal{D}_{L/R} &= \begin{pmatrix} D & XD \end{pmatrix}_{L/R}^T \equiv \begin{pmatrix} d & s & b & xd_1 & xd_2 & xd_3 \end{pmatrix}_{L/R}^T. \end{aligned} \quad (21)$$

The matrices \mathcal{M}^u and \mathcal{M}^d from Eq. 19 will be diagonalized by biunitary transformations and are given by

$$\begin{aligned} \hat{\mathcal{U}}_{L/R} &= S_{L/R}^u \mathcal{U}_{L/R} \\ \hat{\mathcal{D}}_{L/R} &= S_{L/R}^d \mathcal{D}_{L/R}, \end{aligned} \quad (22)$$

where the S_L^u and S_L^d are 6×6 unitary matrices and can be represented by

$$\mathcal{S}_L^u = \begin{pmatrix} A_L^u & E_L^u \\ F_L^u & G_L^u \end{pmatrix}, \quad \mathcal{S}_L^d = \begin{pmatrix} A_L^d & E_L^d \\ F_L^d & G_L^d \end{pmatrix}. \quad (23)$$

The matrices \mathcal{S}_R^u and \mathcal{S}_R^d can be obtained from Eq. 23 by replacing $L \rightarrow R$. The matrices A, E, F, G are 3×3 dimensional and where E and F connect the SM quarks with the VLQs. To avoid FCNC at the tree level we choose the mixing pattern such that the matrices for the left chiral sector take the form

$$A_L^u = \widehat{A}_L^u C_L^u, \quad F_L^u = S_L^u, \quad G_L^u = C_L^u, \quad E_L^u = -\widehat{A}_L^u S_L^u, \quad (24)$$

where

$$\begin{aligned} \widehat{A}_L^{u\dagger} \widehat{A}_L^u &= \widehat{A}_L^u \widehat{A}_L^{u\dagger} = \mathbb{1}, \\ C_L^u &= \text{diag}(\cos \theta_L^u, \cos \theta_L^c, \cos \theta_L^t), \quad S_L^u = \text{diag}(\sin \theta_L^u, \sin \theta_L^c, \sin \theta_L^t), \end{aligned} \quad (25)$$

then,

$$\begin{aligned} u_L &= \cos \theta_L^u \left(\widehat{A}_L^{u\dagger} \begin{pmatrix} u^0 \\ c^0 \\ t^0 \end{pmatrix}_L \right)_1 + \sin \theta_L^u x u_{1L}^0, & x u_{1L} &= -\sin \theta_L^u \left(\widehat{A}_L^{u\dagger} \begin{pmatrix} u^0 \\ c^0 \\ t^0 \end{pmatrix}_L \right)_1 + \cos \theta_L^u x u_{1L}^0, \\ c_L &= \cos \theta_L^c \left(\widehat{A}_L^{u\dagger} \begin{pmatrix} u^0 \\ c^0 \\ t^0 \end{pmatrix}_L \right)_2 + \sin \theta_L^c x u_{2L}^0, & x u_{2L} &= -\sin \theta_L^c \left(\widehat{A}_L^{u\dagger} \begin{pmatrix} u^0 \\ c^0 \\ t^0 \end{pmatrix}_L \right)_2 + \cos \theta_L^c x u_{2L}^0, \\ t_L &= \cos \theta_L^t \left(\widehat{A}_L^{u\dagger} \begin{pmatrix} u^0 \\ c^0 \\ t^0 \end{pmatrix}_L \right)_3 + \sin \theta_L^t x u_{3L}^0, & x u_{3L} &= -\sin \theta_L^t \left(\widehat{A}_L^{u\dagger} \begin{pmatrix} u^0 \\ c^0 \\ t^0 \end{pmatrix}_L \right)_3 + \cos \theta_L^t x u_{3L}^0. \end{aligned} \quad (26)$$

From Eq. 26 it can be seen that each vector like quark mixes with only one linear combination of the SM gauge eigenstate quarks. The different linear combinations with which different VLQs mix are characterized by the unitary matrix \widehat{A}_L^u .

Similarly to avoid FCNC in the down-type quark sector we choose the mixing matrices for the left chiral down-type quarks in a similar way as above with up-types changed with down-type quarks :

$$A_L^d = \widehat{A}_L^d C_L^d, \quad F_L^d = S_L^d, \quad G_L^d = C_L^d, \quad E_L^d = -\widehat{A}_L^d S_L^d \quad (27)$$

where

$$\widehat{A}_L^q \widehat{A}_L^q{}^\dagger = \widehat{A}_L^d \widehat{A}_L^d{}^\dagger = \mathbb{1},$$

$$C_L^d = \text{diag}(\cos \theta_L^d, \cos \theta_L^s, \cos \theta_L^b), \quad S_L^d = \text{diag}(\sin \theta_L^d, \sin \theta_L^s, \sin \theta_L^b). \quad (28)$$

The mixing matrices and the mass eigenstates for the right handed fields can be obtained by replacing $L \rightarrow R$ in Eqs. 24-28. Note that both Eq. 26 and its right handed counterpart show that in the absence of mixing between the SM quarks and the VLQs, the unitary matrices \widehat{A}_L^u and \widehat{A}_R^u are the matrices which diagonalize the mass matrix for the up-quark sector of the SM. The same can be concluded for the down-quark sector also.

A. CKM Matrix in presence of Vector Like Quarks

The interaction of the SM left-chiral gauge eigenstates with the W boson is given by

$$\frac{g_1}{\sqrt{2}} W_\mu^+ \overline{U}_L^0 \gamma^\mu D_L^0 = \frac{g_1}{\sqrt{2}} W_\mu^+ \left\{ \overline{U}_L A_L^{u\dagger} A_L^d \gamma^\mu D_L + \overline{XU}_L E_L^{u\dagger} A_L^d \gamma^\mu D_L \right. \\ \left. + \overline{U}_L A_L^{u\dagger} E_L^d \gamma^\mu XD_L + \overline{XU}_L E_L^{u\dagger} E_L^d \gamma^\mu XD_L \right\}. \quad (29)$$

Based on the interactions of the SM quark mass eigenstates with the W boson the CKM matrix is defined as

$$V_L^{CKM} = A_L^{u\dagger} A_L^d = C_L^u \widehat{A}_L^{u\dagger} \widehat{A}_L^d C_L^d. \quad (30)$$

V_L^{CKM} corresponds to the measured CKM matrix. It can be noted that in the presence of mixing between SM quarks and VLQs the matrix V_L^{CKM} is not unitary. The deviation from unitarity of the measured CKM matrix will put constraints on the mixing angles contained in the matrices C_L^u and C_L^d .

Similarly the interaction term of the SM right-chiral quark gauge eigenstates with the W' gauge boson is given by

$$\frac{g_2}{\sqrt{2}} W_\mu'^+ \overline{U}_R^0 \gamma^\mu D_R^0 = \frac{g_1}{\sqrt{2}} W_\mu'^+ \left\{ \overline{U}_R A_R^{u\dagger} A_R^d \gamma^\mu D_R + \overline{XU}_R E_R^{u\dagger} A_R^d \gamma^\mu D_R \right. \\ \left. + \overline{U}_R A_R^{u\dagger} E_R^d \gamma^\mu XD_R + \overline{XU}_R E_R^{u\dagger} E_R^d \gamma^\mu XD_R \right\}. \quad (31)$$

We define a right-handed CKM matrix given by

$$V_R^{CKM} = A_R^{u\dagger} A_R^d = C_R^u \widehat{A}_R^{u\dagger} \widehat{A}_R^d C_R^d. \quad (32)$$

B. FCNC interaction with Z and Z'

To see how the choice of mixing pattern that we have considered avoids FCNC at tree level, we focus on the terms containing Z boson in Eq. 18. Since all the fields u_L^0 , c_L^0 and t_L^0

carry universal charges under the full gauge group, we can write their interaction with the Z boson in terms of U^0 of Eq. 21 as

$$\frac{e}{\sin \theta_W \cos \theta_W} \left\{ \left(\frac{1}{2} - \frac{2}{3} \sin^2 \theta_W \right) - \frac{1}{6} \epsilon \cos^2 \phi \sin^2 \phi \right\} Z_\mu \overline{U}_L^0 \gamma^\mu U_L^0. \quad (33)$$

The flavour diagonal nature can be seen by writing $\overline{U}_L^0 \gamma^\mu U_L^0$ in terms of mass eigenstates by using the Eqs. 21-24 and is given by

$$\overline{U}_L^0 \gamma^\mu U_L^0 = \overline{U}_L C_L^{u2} \gamma^\mu U_L - (\overline{U}_L C_L^u S_L^u \gamma^\mu X U_L + \overline{X U}_L S_L^u C_L^u \gamma^\mu U_L) + \overline{X U}_L S_L^{u2} \gamma^\mu X U_L. \quad (34)$$

Since C_L^u is a diagonal matrix, the first term in the right hand side of the above equation is diagonal in the mass eigenstates u_L , c_L and t_L . Similarly, with the equivalent form of Eq.34 for U_R^0 , $X U_{L/R}^0$, $D_{L/R}^0$ and $X D_{L/R}^0$, and since S_L^u is also a diagonal matrix, we find that there is no flavour-changing interactions of the SM quarks with the Z boson. Again, by expanding the interaction terms for Z' in Eq. 18 we find that the Z' also does not have any flavour-changing interactions with the SM quarks for the chosen mixing pattern.

C. FCNH interaction with Higgs Bosons

The unitary matrices in Eq. 22 diagonalize the quark mass matrices, i.e.,

$$\begin{aligned} \mathcal{S}_L^{u\dagger} \begin{pmatrix} \frac{1}{\sqrt{2}}(Y^q v_1 + Y^{qC} v_2^*) & Y^{qxu} \frac{v_3}{\sqrt{2}} \\ \mu & Y^{xqxu} \frac{u}{\sqrt{2}} \end{pmatrix} \mathcal{S}_R^u &= \mathcal{M}_{diag}^u, \\ \mathcal{S}_L^{d\dagger} \begin{pmatrix} \frac{1}{\sqrt{2}}(Y^q v_2 + Y^{qC} v_1^*) & Y^{qxd} \frac{v_3}{\sqrt{2}} \\ \mu & Y^{xqxd} \frac{u}{\sqrt{2}} \end{pmatrix} \mathcal{S}_R^d &= \mathcal{M}_{diag}^d, \end{aligned} \quad (35)$$

where

$$\mathcal{M}_{diag}^u = \begin{pmatrix} M_{diag}^u & 0 \\ 0 & M_{diag}^{xu} \end{pmatrix} \quad \text{and} \quad \mathcal{M}_{diag}^d = \begin{pmatrix} M_{diag}^d & 0 \\ 0 & M_{diag}^{xd} \end{pmatrix}. \quad (36)$$

And

$$\begin{aligned} M_{diag}^u &= \text{diag}(m_u, m_c, m_t), \quad M_{diag}^d = \text{diag}(m_d, m_s, m_b), \\ M_{diag}^{xu} &= \text{diag}(m_{xu_1}, m_{xu_2}, m_{xu_3}), \quad M_{diag}^{xd} = \text{diag}(m_{xd_1}, m_{xd_2}, m_{xd_3}). \end{aligned} \quad (37)$$

From Eq. 35 the Yukawa couplings with the bi-doublet in terms of mixing matrices are given by

$$\begin{aligned} \frac{1}{\sqrt{2}}(Y^q v_1 + Y^{qC} v_2^*) &= A_L^u M_{diag}^u A_R^{u\dagger} + E_L^u M_{diag}^{xu} E_R^{u\dagger}, \\ \frac{1}{\sqrt{2}}(Y^q v_2 + Y^{qC} v_1^*) &= A_L^d M_{diag}^d A_R^{d\dagger} + E_L^d M_{diag}^{xd} E_R^{d\dagger}. \end{aligned} \quad (38)$$

Solving Eq. 38 for Y^q and Y^{qC} we get

$$\begin{aligned} Y^q &= \frac{\sqrt{2}}{|v_1|^2 - |v_2|^2} \left(v_1^* (A_L^u M_{diag}^u A_R^{u\dagger} + E_L^u M_{diag}^{xu} E_R^{u\dagger}) - v_2^* (A_L^d M_{diag}^d A_R^{d\dagger} + E_L^d M_{diag}^{xd} E_R^{d\dagger}) \right), \\ Y^{qC} &= \frac{\sqrt{2}}{|v_1|^2 - |v_2|^2} \left(-v_2 (A_L^u M_{diag}^u A_R^{u\dagger} + E_L^u M_{diag}^{xu} E_R^{u\dagger}) + v_1 (A_L^d M_{diag}^d A_R^{d\dagger} + E_L^d M_{diag}^{xd} E_R^{d\dagger}) \right). \end{aligned} \quad (39)$$

From the Yukawa Lagrangian in Eq. 4 the interaction of the neutral components of the bi-doublet Φ with the SM quarks in the gauge basis is given by

$$\overline{U}_L^0 (Y^q \phi_1^0 + Y^{qC} \phi_2^{0*}) U_R^0 + \overline{D}_L^0 (Y^q \phi_2^0 + Y^{qC} \phi_1^{0*}) D_R^0. \quad (40)$$

Using Eq. 39 and Eqs. 22-28 the interactions of the scalars ϕ_1^0 and ϕ_2^0 with the SM up type quarks in the mass basis can be written as

$$\begin{aligned} &\overline{U}_L A_L^{u\dagger} (Y^q \phi_1^0 + Y^{qC} \phi_2^{0*}) A_R^u U_R \\ &= \frac{\sqrt{2}}{v_-^2} \overline{U}_L \left((v_1^* \phi_1^0 - v_2 \phi_2^{0*}) (C_L^{u2} M_{diag}^u C_R^{u2} + C_L^u S_L^u M_{diag}^{xu} S_R^u C_R^u) \right. \\ &\quad \left. + (-v_2^* \phi_1^0 + v_1 \phi_2^{0*}) (V_L^{CKM} M_{diag}^d V_R^{CKM\dagger} + A_L^{u\dagger} E_L^d M_{diag}^{xd} E_R^{d\dagger} A_R^u) \right) U_R \\ &= \frac{\sqrt{2}}{v_-^2} \overline{U}_L \left(\phi_-^0 \frac{v_-^2}{v_+} (C_L^{u2} M_{diag}^u C_R^{u2} + C_L^u S_L^u M_{diag}^{xu} S_R^u C_R^u) \right. \\ &\quad \left. + \phi_+^0 \left\{ \frac{-2v_1^* v_2}{v_+} (C_L^{u2} M_{diag}^u C_R^{u2} + C_L^u S_L^u M_{diag}^{xu} S_R^u C_R^u) \right. \right. \\ &\quad \left. \left. + v_+ (V_L^{CKM} M_{diag}^d V_R^{CKM\dagger} + V_L^{CKM} C_L^{-1} S_L^d M_{diag}^{xd} S_R^d C_R^{-1} V_R^{CKM\dagger}) \right\} \right) U_R, \end{aligned} \quad (41)$$

where the two orthogonal fields ϕ_-^0 and ϕ_+^0 are given by[52]

$$\begin{aligned} \phi_+^0 &= \frac{1}{v_+} (-v_2^* \phi_1^0 + v_1 \phi_2^{0*}), \\ \phi_-^0 &= \frac{1}{v_+} (v_1^* \phi_1^0 + v_2 \phi_2^{0*}). \end{aligned} \quad (42)$$

And $v_{\pm}^2 = |v_1|^2 \pm |v_2|^2$. Similarly the interaction terms for the SM down type quarks in the mass basis is given by

$$\begin{aligned} &\overline{D}_L A_L^{d\dagger} (Y^q \phi_2^0 + Y^{qC} \phi_1^{0*}) A_R^d D_R \\ &= \frac{\sqrt{2}}{v_-^2} \overline{D}_L \left(\phi_-^{0*} \frac{v_-^2}{v_+} (C_L^{d2} M_{diag}^d C_R^{d2} + C_L^d S_L^d M_{diag}^{xd} S_R^d C_R^d) \right. \\ &\quad \left. + \phi_+^{0*} \left\{ \frac{-2v_1 v_2^*}{v_+} (C_L^{d2} M_{diag}^d C_R^{d2} + C_L^d S_L^d M_{diag}^{xd} S_R^d C_R^d) \right. \right. \\ &\quad \left. \left. + v_+ (V_L^{CKM\dagger} M_{diag}^u V_R^{CKM} + V_L^{CKM\dagger} C_L^{u-1} S_L^u M_{diag}^{xu} S_R^u C_R^{u-1} V_R^{CKM}) \right\} \right) D_R. \end{aligned} \quad (43)$$

From Eq. 41 and Eq. 43 it can be concluded that the interactions ϕ_-^0 is flavour-diagonal but the interactions of ϕ_+^0 is flavour-changing. ϕ_+^0 interactions are flavour-changing because the matrix V_L^{CKM} which is the measured CKM matrix is not diagonal. Although the matrix V_R^{CKM} can be non-diagonal there is no experimental constraint which forces it to be non-diagonal and hence V_R^{CKM} can be taken to be diagonal by proper choice of Yukawa couplings. In left-right symmetric model the field ϕ_-^0 is always flavour-conserving in nature [52]. But in the 221 model we are discussing ϕ_-^0 can also have flavour-violating interactions for general mixing patterns between VLQs and the SM quarks. It is the form of the mixing matrices in Eq. 24 and Eq. 27 which ensures that ϕ_-^0 have flavour-conserving interactions.

In general ϕ_+^0 is not a mass eigenstate and when both v_1 and v_2 are nonzero all the neutral mass eigenstates will contain ϕ_+^0 . And hence all of the neutral scalars have to be heavy to avoid constraints from FCNC interactions. Therefore when both v_1 and v_2 take nonzero values it will be impossible to get a light mass eigenstate at 125 GeV which do not have flavour violating interactions. This scenario has been extensively discussed in the context of left-right symmetric model in [53].

Hence to have a flavour-conserving Higgs at 125 GeV we made the choice $v_2 = 0$, which gives

$$v_+ = v_- = v_1, \quad \phi_+^0 = \phi_2^{0*}, \quad \phi_-^0 = \phi_1^0. \quad (44)$$

The VEV v_1 has been considered as a real parameter. As we will show it is possible to choose the parameters of the scalar potential in the model such that ϕ_2^0 do not mix with any other scalars and can be made heavy to avoid large neutral flavour-changing interactions. ϕ_1^0 will be a part of the observed 125 GeV Higgs. For $v_2 = 0$ the interactions of flavour conserving Higgs ϕ_1^0 with the SM type quarks are given by

$$\begin{aligned} & \frac{\sqrt{2}}{v_1} \overline{U}_L \left(\phi_1^0 (C_L^{u2} M_{\text{diag}}^u C_R^{u2} + C_L^u S_L^u M_{\text{diag}}^{xu} S_R^u C_R^u) \right) U_R + \text{H.C.}, \\ & \frac{\sqrt{2}}{v_1} \overline{D}_L \left(\phi_1^{0*} (C_L^{d2} M_{\text{diag}}^d C_R^{d2} + C_L^d S_L^d M_{\text{diag}}^{xd} S_R^d C_R^d) \right) D_R + \text{H.C.} \end{aligned} \quad (45)$$

And the interactions for the flavour-violating Higgs ϕ_2^0 are given by

$$\begin{aligned} & \frac{\sqrt{2}}{v_1} \overline{U}_L \left(\phi_2^0 \left\{ (V_L^{\text{CKM}} M_{\text{diag}}^d V_R^{CKM\dagger} + A_L^{u\dagger} E_L^d M_{\text{diag}}^{xd} E_R^{d\dagger} A_R^u) \right\} \right) U_R + \text{H.C.}, \\ & \frac{\sqrt{2}}{v_1} \overline{D}_L \left(\phi_2^0 \left\{ (V_L^{\text{CKM}\dagger} M_{\text{diag}}^u V_R^{CKM} + A_L^{d\dagger} E_L^u M_{\text{diag}}^{xu} E_R^{u\dagger} A_R^d) \right\} \right) D_R + \text{H.C.} \end{aligned} \quad (46)$$

To study the nature of interactions of the neutral components from the doublets H_1 and H_2 we list the Yukawa couplings in terms of the mixing matrices as below (for mixing

matrices of the form taken in Eq. 24 and $v_2 = 0$)

$$\begin{aligned}
Y^q \frac{v_1}{\sqrt{2}} &= \widehat{A}_L^u \left(C_L^u M_{diag}^u C_R^u + S_L^u M_{diag}^{xu} S_R^u \right) \widehat{A}_R^{u\dagger}, \\
Y^{qxu} \frac{v_3}{\sqrt{2}} &= \widehat{A}_L^u \left(C_L^u M_{diag}^u S_R^u - S_L^u M_{diag}^{xu} C_R^u \right), \\
\mu &= (S_L^u M_{diag}^u C_R^u - C_L^u M_{diag}^{xu} S_R^u) \widehat{A}_R^{u\dagger}, \\
Y^{xqxu} \frac{u}{\sqrt{2}} &= S_L^u M_{diag}^u S_R^u + C_L^u M_{diag}^{xu} C_R^u.
\end{aligned} \tag{47}$$

Similar relations for the matrices Y^{qC} , Y^{qxd} , μ and Y^{xqxd} can be found by using the mixing matrices for the down-type quark sector. Note that the mixing angles and the mass eigenvalues should be such that both the up-quark sector and the down-quark sector yield the same μ matrix.

The fields χ^0 and χ'^0 in Eq. 7 are the neutral components of the doublets H_1 and H_2 respectively. The interactions of the up-type SM mass eigenstate quarks with χ^0 and χ'^0 can be derived from the terms proportional to Y_{ij}^{qxu} and Y_{ij}^{xqxu} respectively in the Yukawa Lagrangian. These interactions are given by

$$\begin{aligned}
Y_{ij}^{qxu} \overline{Q_{iL}} x u_{jR}^0 H_1 &\supset \chi^0 \overline{U_L^0} Y^{qxu} X U_R^0 \\
&\supset \frac{\sqrt{2}}{v_3} \chi^0 \overline{U_L} \left[C_L^u \left(C_L^u M_{diag}^u S_R^u - S_L^u M_{diag}^{xu} C_R^u \right) S_R^u \right] U_R \\
\text{and } Y_{ij}^{xqxu} \overline{X Q_{iL}} x u_{jR}^0 H_2 &\supset \chi'^0 \overline{X U_L^0} Y^{xqxu} X U_R^0 \\
&\supset \frac{\sqrt{2}}{u} \chi'^0 \overline{U_L} \left[S_L^u \left(S_L^u M_{diag}^u S_R^u + C_L^u M_{diag}^{xu} C_R^u \right) S_R^u \right] U_R.
\end{aligned} \tag{48}$$

The superset sign (\supset) has been used in the above equations to highlight the terms containing only the fields χ^0 , χ'^0 and the SM up-type mass eigenstate quarks (U_L, U_R). From Eq. 48 it can be concluded that the scalars χ^0 and χ'^0 do not have flavour changing interactions with the SM mass eigenstate quarks.

Based on the above discussions, we denote the field ϕ_2^0 as the FCNH (flavour-changing neutral Higgs) scalar and the fields ϕ_1^0 , χ^0 and χ'^0 as the three non-FCNH scalars in the model. One linear combination of the three non-FCNH scalars will be the 125 GeV SM Higgs and the other linear combinations can lie at the sub-TeV scale.

The special cases for the matrices Y^{qxu} and μ which will play an important role in the phenomenology of the VLQs are given by :

$$Y^{qxu} = 0 \implies \tan \theta_L^i = \frac{m_i}{m_{xu_i}} \tan \theta_R^i \tag{49}$$

and

$$\mu = 0 \implies \tan \theta_R^i = \frac{m_i}{m_{xu_i}} \tan \theta_L^i, \tag{50}$$

where $i \in (u, c, t)$.

For simplicity we consider the scenario where the three matrices \widehat{A}_L^d , \widehat{A}_R^u and \widehat{A}_R^d are equal to $\mathbb{1}$. The choice for the Yukawa couplings which will lead to such a scenario can be made by using $\widehat{A}_L^d = \mathbb{1}$, $\widehat{A}_R^u = \mathbb{1}$ and $\widehat{A}_R^d = \mathbb{1}$ in Eq. 47. From Eq. 47 it can be observed that the complete determination of Yukawa couplings will depend on the SM quark masses, desired values of VLQ masses, desired values of mixing angles, VEVs and on the form of the matrix \widehat{A}_L^u . The measured CKM matrix will enter through the matrix \widehat{A}_L^u because, $V_L^{\text{CKM}} = A_L^{u\dagger} A_L^d = C_L^u \widehat{A}_L^{u\dagger} \widehat{A}_L^d C_L^d$.

V. PHENOMENOLOGICAL ASPECTS

So far we have discussed about the methodology to get rid of any tree level Z boson FCNC and to achieve a 125 GeV Higgs with no flavor changing interactions. Now we shall discuss some of the phenomenological implications of the model. To do that we will choose a representative mass spectrum for the exotic particles in our model and then discuss the possible collider signals which can be explored at the LHC.

A. Scalar and gauge boson mass spectrum

To relate the gauge eigenstates with the mass eigenstates for the scalar sector, we introduce three 4×4 matrices Z^E , Z^O and Z^C for CP even sector, CP odd sector and charged sector respectively. The relations are given by

$$\begin{pmatrix} h_1 \\ h_2 \\ h_3 \\ h_4 \end{pmatrix} = Z^E \begin{pmatrix} \phi_1^{0r} \\ \phi_2^{0r} \\ \chi'^{0r} \\ \chi^{0r} \end{pmatrix}, \quad \begin{pmatrix} G_1 \\ G_2 \\ A_1 \\ A_2 \end{pmatrix} = Z^O \begin{pmatrix} \phi_1^{0i} \\ \phi_2^{0i} \\ \chi'^{0i} \\ \chi^{0i} \end{pmatrix}, \quad \begin{pmatrix} G_1^+ \\ G_2^+ \\ h_1^+ \\ h_2^+ \end{pmatrix} = Z^C \begin{pmatrix} \phi_1^+ \\ \phi_2^+ \\ \chi'^+ \\ \chi^+ \end{pmatrix}. \quad (51)$$

Here h_1, h_2, h_3, h_4 are CP even scalar mass eigenstates, A_1 and A_2 are CP odd scalar mass eigenstates and h_1^+, h_2^+ are charged scalar mass eigenstates. G_1, G_2 are neutral Goldstone bosons and G_1^+, G_2^+ are the charged Goldstone bosons. As discussed in the previous section, the field ϕ_2^0 will have FCNH interactions while the fields ϕ_1^0, χ^0 and χ'^0 have no FCNH interactions. Therefore, any mass eigenstate formed out of the linear combinations of the three fields ϕ_1^0, χ^0 and χ'^0 can lie at sub-TeV scale. A typical example of the composition of the sub-TeV scalar states can be arranged through the following choice of the parameter

values in our model:

$$\begin{aligned} \{M_2, \alpha_1, \alpha_2, \beta_1, \beta_2, \lambda_2, \lambda_3, \lambda_4, \rho_3\} &= 0, \\ u &= 12 \text{ TeV}, M_1 = -0.3 \text{ GeV}, v_2 = 0, v_3 = 7 \text{ GeV}, \\ \rho_1 &= 0.1, \rho_2 = 1, \lambda_1 = 0.13, \beta_3 = 1.4 \text{ and } \alpha_3 = 1. \end{aligned}$$

For the above choice of parameters the mixing matrices are given by

$$\begin{aligned} Z^E &= \begin{pmatrix} 0.999 & 0 & \sim 10^{-8} & 0.034 \\ -0.034 & 0 & \sim 10^{-7} & 0.999 \\ 0 & 1 & 0 & 0 \\ \sim -10^{-8} & 0 & \sim 1 & \sim -10^{-7} \end{pmatrix}, \quad Z^O = \begin{pmatrix} 0.999 & 0 & 0.02 & 0.028 \\ -0.02 & 0 & 0.999 & 0 \\ -0.028 & 0 & \sim -10^{-4} & 0.999 \\ 0 & 1 & 0 & 0 \end{pmatrix}, \\ & \hspace{15em} (52) \\ Z^C &= \begin{pmatrix} 0.999 & 0 & 0 & 0.028 \\ 0 & 0.02 & 0.999 & 0 \\ -0.028 & 0 & 0 & 0.999 \\ 0 & 0.999 & -0.02 & 0 \end{pmatrix}. \end{aligned}$$

The mass eigenvalues are : $m_{h_1} \approx 125 \text{ GeV}$, $m_{h_2} \approx 300 \text{ GeV}$, $m_{h_3} \approx 8.5 \text{ TeV}$, $m_{h_4} \approx 17 \text{ TeV}$, $m_{A_1} \simeq 300 \text{ GeV}$, $m_{A_2} \simeq 8.5 \text{ TeV}$, $m_{h_1^+} \simeq 363 \text{ GeV}$ and $m_{h_2^+} \simeq 8.5 \text{ TeV}$. We shall keep this spectrum for the scalars as our choice for the collider analysis presented later.

The mixing matrices clearly show that the neutral scalars h_3 and A_2 , which are basically ϕ_2^{0r} and ϕ_2^{0i} respectively, have been kept unmixed with other neutral scalars, because both ϕ_2^{0r} and ϕ_2^{0i} have FCNH interactions as discussed earlier.

For the choice $u = 12 \text{ TeV}$ and for $g_2 = g_1$, the mass values for W' and Z' are $M_{W'} \simeq 4 \text{ TeV}$ and $M_{Z'} \simeq 4.7 \text{ TeV}$ respectively, and both of them satisfies the current lower bounds obtained by the ATLAS collaboration [54, 55]. Also the $Z - Z'$ mixing angle is small ($\theta_{zz'} \simeq 10^{-4}$) and satisfies the constraint from the electroweak precision data [56]. Note that for $v_2 = 0$, the $W - W'$ mixing angle $\theta_{ww'}$ (see Eq. 14) is zero.

B. Production and decay of the Vector Like Quarks

As color triplets, the VLQs will be pair-produced at the LHC mostly through strong interactions. The pair production cross section at LHC with different center-of-mass energies and as a function of the mass of xu_3 has been shown in fig.1. We have used NN23L01[57] parton distribution function with default factorization and renormalization scale in Madgraph5_aMC@NLO for our estimates.

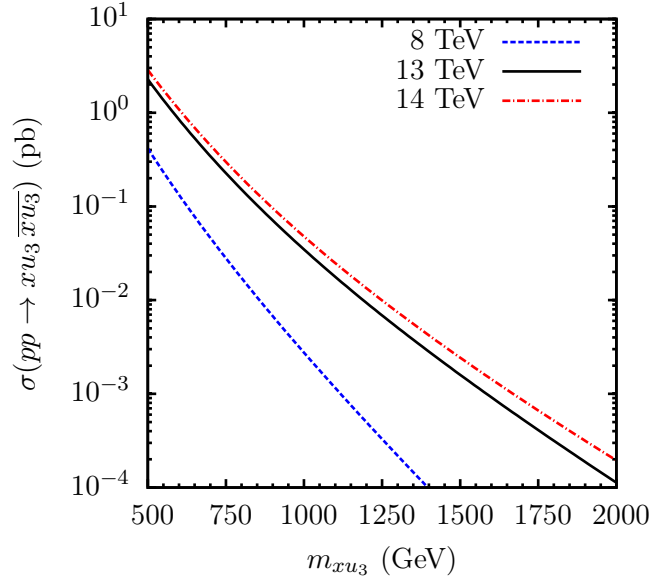


FIG. 1: Production cross section for the VLQ xu_3 for different masses for 8 TeV, 13 TeV and 14 TeV LHC.

For a given set of allowed values for the parameters in the model, the six VLQs (three up-type and three down-type) will mostly have different signatures depending on the generation they belong to. To discuss the phenomenology and for simplicity we consider the third generation up-type VLQ xu_3 to be the lightest one among all VLQs in the model. Since we have already discussed in detail the mixing between VLQs and SM quarks, we list the relevant interaction terms for xu_3 in table 2. As the interactions with the physical scalar fields would look quite cumbersome and messy, we have chosen to show the interaction of the physical (mass eigenstates) fermions with the scalars in the gauge eigenbasis. The interaction terms with the physical scalars can be obtained by using the rotated fields in terms of the elements of 4×4 matrices Z^E , Z^O and Z^C . For example, the interaction term for A_1 will be

$$A_1 \bar{t} x u_3 : \left[(Z^O)_{13}^T K_{\phi_1^{0i}} (C_{\phi_1^{0i}}^S + C_{\phi_1^{0i}}^P \gamma^5) + (Z^O)_{23}^T K_{\phi_2^{0i}} (C_{\phi_2^{0i}}^S + C_{\phi_2^{0i}}^P \gamma^5) \right. \\ \left. + (Z^O)_{33}^T K_{\chi'^{0i}} (C_{\chi'^{0i}}^S + C_{\chi'^{0i}}^P \gamma^5) + (Z^O)_{43}^T K_{\chi^{0i}} (C_{\chi^{0i}}^S + C_{\chi^{0i}}^P \gamma^5) \right].$$

The possible final states that xu_3 can decay to are tZ , th_1 , bW^+ , th_2 , tA_1 and bh_1^+ , since the scalars h_3 , h_4 , A_2 , h_2^+ and the new gauge bosons Z' , W' are heavier compared to the VLQ xu_3 . For small mixing angles the “non-standard” decay modes (th_2 , tA_1 , bh_1^+) will mostly dominate over the standard decay modes (tZ , th_1 , bW^+) because of the presence of direct Yukawa interaction term, Y^{qu} in the Lagrangian. The standard decay modes will

$\phi \bar{t} x u_3$	K_ϕ	C_ϕ^S	C_ϕ^P
$\phi_1^{0r} \bar{t} x u_3$	$-\frac{1}{2v_1}(c_L^t m_t c_R^t + s_L^t m_{xu_3} s_R^t)$	$c_L^t s_R^t + s_L^t c_R^t$	$c_L^t s_R^t - s_L^t c_R^t$
$\phi_2^{0r} \bar{t} x u_3$	$-\frac{1}{2v_1}(c_L^b m_b c_R^b + s_L^b m_{xd_3} s_R^b)$	$(V_L^{CKM})_{tb} \frac{s_R^t}{c_L^b}$ + $(V_L^{CKM*})_{tb} \frac{c_R^t s_L^t}{c_L^b c_L^t}$	$(V_L^{CKM})_{tb} \frac{s_R^t}{c_L^b}$ - $(V_L^{CKM*})_{tb} \frac{c_R^t s_L^t}{c_L^b c_L^t}$
$\chi^{0r} \bar{t} x u_3$	$\frac{1}{2v_3}(c_L^t m_t s_R^t - s_L^t m_{xu_3} c_R^t)$	$c_L^t c_R^t - s_L^t s_R^t$	$c_L^t c_R^t + s_L^t s_R^t$
$\chi'^{0r} \bar{t} x u_3$	$\frac{1}{2u}(s_L^t m_t s_R^t + c_L^t m_{xu_3} c_R^t)$	$s_L^t c_R^t + c_L^t s_R^t$	$s_L^t c_R^t - c_L^t s_R^t$
$\phi_1^{0i} \bar{t} x u_3$	$-\frac{i}{2v_1}(c_L^t m_t c_R^t + s_L^t m_{xu_3} s_R^t)$	$c_L^t s_R^t - s_L^t c_R^t$	$c_L^t s_R^t + s_L^t c_R^t$
$\phi_2^{0i} \bar{t} x u_3$	$\frac{i}{2v_1}(c_L^b m_b c_R^b + s_L^b m_{xd_3} s_R^b)$	$(V_L^{CKM})_{tb} \frac{s_R^t}{c_L^b}$ - $(V_L^{CKM*})_{tb} \frac{c_R^t s_L^t}{c_L^b c_L^t}$	$(V_L^{CKM})_{tb} \frac{s_R^t}{c_L^b}$ + $(V_L^{CKM*})_{tb} \frac{c_R^t s_L^t}{c_L^b c_L^t}$
$\chi^{0i} \bar{t} x u_3$	$\frac{i}{2v_3}(c_L^t m_t s_R^t - s_L^t m_{xu_3} c_R^t)$	$c_L^t c_R^t + s_L^t s_R^t$	$c_L^t c_R^t - s_L^t s_R^t$
$\chi'^{0i} \bar{t} x u_3$	$\frac{i}{2u}(s_L^t m_t s_R^t + c_L^t m_{xu_3} c_R^t)$	$s_L^t c_R^t - c_L^t s_R^t$	$s_L^t c_R^t + c_L^t s_R^t$
$\phi_1^- \bar{b} x u_3$	$\frac{1}{\sqrt{2}v_1}$	$-s_L^t c_R^b(c_L^t m_t c_R^t + s_L^t m_{xu_3} s_R^t)$ + $c_L^b s_R^t(c_L^b m_b c_R^b + s_L^b m_{xd_3} s_R^b)$	$s_L^t c_R^b(c_L^t m_t c_R^t + s_L^t m_{xu_3} s_R^t)$ + $c_L^b s_R^t(c_L^b m_b c_R^b + s_L^b m_{xd_3} s_R^b)$
$\phi_2^- \bar{b} x u_3$	$\frac{(V_L^{CKM*})_{tb}}{\sqrt{2}v_1}$	$-\frac{s_R^t}{c_L^t}(c_L^t m_t c_R^t + s_L^t m_{xu_3} s_R^t)$ + $\frac{s_L^t c_R^b}{c_L^t c_L^b}(c_L^b m_b c_R^b + s_L^b m_{xd_3} s_R^b)$	$-\frac{s_R^t}{c_L^t}(c_L^t m_t c_R^t + s_L^t m_{xu_3} s_R^t)$ - $\frac{s_L^t c_R^b}{c_L^t c_L^b}(c_L^b m_b c_R^b + s_L^b m_{xd_3} s_R^b)$
$\chi^- \bar{b} x u_3$	$\frac{(V_L^{CKM*})_{tb}}{\sqrt{2}v_3}$	$\frac{c_R^t}{c_L^t}(c_L^t m_t s_R^t - s_L^t m_{xu_3} c_R^t)$ + $\frac{s_R^b s_L^t}{c_L^b c_L^t}(c_L^b m_b s_R^b - s_L^b m_{xd_3} c_R^b)$	$\frac{c_R^t}{c_L^t}(c_L^t m_t s_R^t - s_L^t m_{xu_3} c_R^t)$ - $\frac{s_R^b s_L^t}{c_L^b c_L^t}(c_L^b m_b s_R^b - s_L^b m_{xd_3} c_R^b)$
$\chi'^- \bar{b} x u_3$	$\frac{1}{\sqrt{2}u}$	$s_L^b c_R^t(s_L^t m_t s_R^t + c_L^t m_{xu_3} c_R^t)$ - $c_L^t s_R^b(s_L^b m_b s_R^b + c_L^b m_{xd_3} c_R^b)$	$s_L^b c_R^t(s_L^t m_t s_R^t + c_L^t m_{xu_3} c_R^t)$ + $c_L^t s_R^b(s_L^b m_b s_R^b + c_L^b m_{xd_3} c_R^b)$
$a_\mu \bar{t} x u_3$	K_a	C_a^V	C_a^A
$Z_\mu \bar{t} x u_3$	$\frac{g}{4 \cos \theta_W}$	$-s_L^t c_L^t$	$s_L^t c_L^t$
$W_\mu^- \bar{b} x u_3$	$\frac{g}{2\sqrt{2}}(V_L^{CKM*})_{tb}$	$\frac{-s_L^t}{c_L^t}$	$\frac{s_L^t}{c_L^t}$

TABLE 2: The interaction terms including scalars are of the form $\phi K_\phi(C_\phi^S + C_\phi^P \gamma^5) x u_3$ and including gauge bosons are of the form $a_\mu \bar{t} K_a \gamma^\mu (C_a^V + C_a^A \gamma^5) x u_3$. The interactions for the physical scalars can be obtained using the transformations given by Eq. 51.

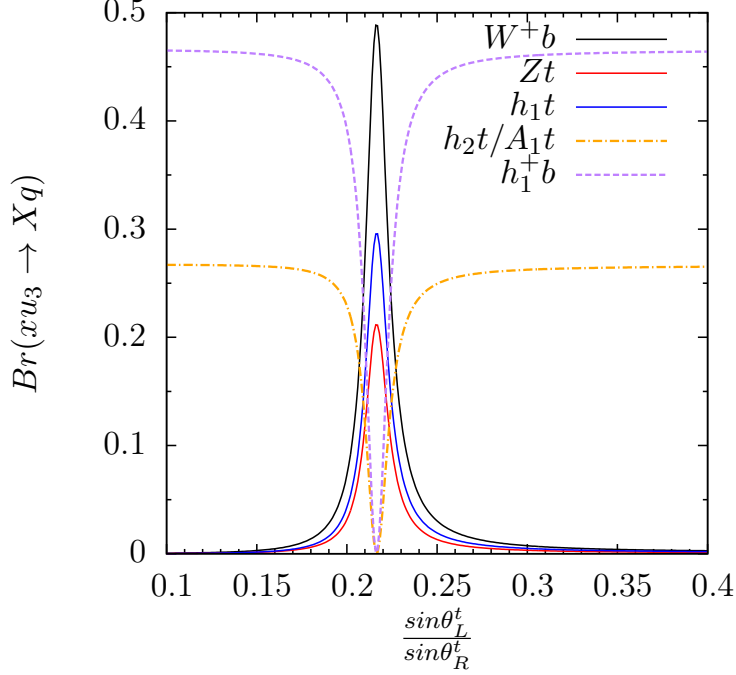


FIG. 2: Branching ratios for different decay modes of the VLQ xu_3 as a function of mixing angle θ_L^t . For the plot $m_{xu_3} = 800$ GeV, $m_{h_2} = m_{A_1} = 300$ GeV, $m_{h_1^+} = 363$ GeV, $m_{x_{d3}} = 5$ TeV, $\sin \theta_L^b = 10^{-4}$, $\sin \theta_R^b \simeq 10^{-4}$ and $\sin \theta_R^t = 10^{-3}$.

start dominating once Y^{qu} tends to zero. This feature is illustrated in Fig. 2 which shows the branching ratios for different decay modes for a 800 GeV xu_3 as function of mixing angles, where we have fixed $\sin \theta_R^t = 10^{-3}$ and varied $\sin \theta_L^t$ accordingly.

We have considered small mixing angles ($\simeq 10^{-3}$) to avoid constraints from flavour sector and electroweak precision data [16, 38–42] and as an example, we have checked that the contribution of VLQs to the $K - \bar{K}$ oscillation parameter Δm_K is few orders of magnitude less compared to the SM value. We find that the non-standard decay modes dominate the standard decay modes except where $\frac{\sin \theta_L^t}{\sin \theta_R^t}$ lies in the small range 0.2-0.23. We can understand this feature of the decay probability by looking at the interaction terms $\chi^{0r} \bar{t} xu_3$, $\chi^{0i} \bar{t} xu_3$ and $\chi^- \bar{b} xu_3$ from Table 2. In the limit $\frac{\tan \theta_L^t}{\tan \theta_R^t} = \frac{m_t}{m_{xu_3}}$, the coupling strengths for the interactions $\chi^{0r} \bar{t} xu_3$ and $\chi^{0i} \bar{t} xu_3$ is identically zero. Moreover, the same limit along with small values of $\sin \theta_L^t$ and $\sin \theta_R^b$ make the coupling strength for the interaction $\chi^- \bar{b} xu_3$ negligibly small. Thus when the ratio of mixing angles become

$$\frac{\sin \theta_L^t}{\sin \theta_R^t} \simeq \frac{\tan \theta_L^t}{\tan \theta_R^t} = \frac{m_t}{m_{xu_3}} \simeq \frac{173}{800} \simeq 0.216, \quad (53)$$

the interactions with the scalars h_2 , A_1 and h_1^+ goes to zero. Consequently the decays of xu_3 to the SM particles enhances. In the next section we study the possible collider signatures for the scenario where the branching ratios for the VLQ xu_3 lie away from the standard mode dominated region such that after production xu_3 decays to one of the final states from $t h_2$, $t A_1$, $b h_1^+$.

The collider signatures of xu_3 will eventually depend on the decay modes of the the scalars h_2 , A_1 and h_1^+ . From Eq. 51 and Eq. 52 we note that the scalar h_2 is made up of a very small component ($\sim 10^{-2}$) of one of the real neutral part of the bi-doublet Higgs field (ϕ_1^{0r}) and a large component of the real neutral part of H_1 , i.e., χ^{0r} . From the Yukawa terms in the Lagrangian it can be seen that H_1 gives mass to the charged leptons but there is no Yukawa interaction term involving SM quarks and H_1 . Hence the strength of the Yukawa interaction for the mass eigenstate h_2 with the SM quarks is negligible compared to the coupling strength with the leptons. Hence h_2 will mostly decay to leptons compared to the SM quarks. The same argument is also applicable for A_1 and h_1^+ , because all of them are largely composed of H_1 . Note that the charged leptons get masses from the VEV of the $SU(2)_L$ doublet scalar H_1 which gets a small VEV, $\frac{v_3}{\sqrt{2}} \sim 5$ GeV. The Yukawa coupling strengths for the scalars h_2 , A_1 , h_1^+ with the leptons from different generations follow the mass hierarchy and with more than 99% probability the scalar h_2 and A_1 will decay to $\tau^+ \tau^-$ whereas h_1^+ will decay to $\tau^+ \nu_\tau$.

C. Benchmark points

For the collider analysis we have chosen three benchmark points based on xu_3 mass. The pair production cross section and the branching ratios for different benchmarks are given in table 3. For all the three cases the masses for the scalars h_2 , A_1 and h_1^+ are kept fixed at 300 GeV, 300 GeV and 363 GeV respectively. Due to the smallness of the Yukawa couplings with the SM quarks, the scalars h_2 and A_2 can not be produced efficiently at the LHC via gluon fusion and the production cross sections of them are few tens of fb for 13 TeV center of mass energy. Hence, the experimental limits on their masses are fairly weak. Note that the Yukawa couplings of these scalars with the VLQs are also very small and the VLQ loops contribute very less towards their production. The scenario is almost same as the lepton-specific two-Higgs doublet model where the limit on the massive states are of the order of 180-200 GeV [58]. Since the production cross-section falls off rapidly for higher masses we have used an integrated luminosity of 100 fb^{-1} for BP1 whereas 3000 fb^{-1} luminosity is used for the analysis of BP2 and BP3.

We would like to emphasise that the benchmark points chosen here are fairly general as

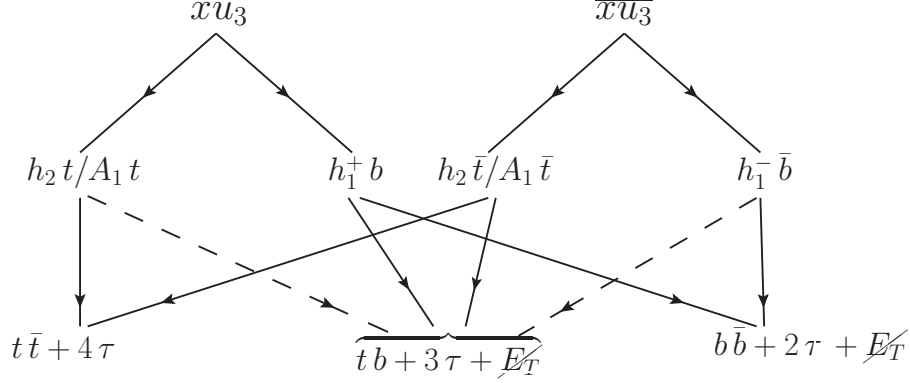


FIG. 3: All possible final states resulting from the pair production of xu_3 and their subsequent non-standard decay.

long as the mass of xu_3 is greater than the masses of the scalars h_2 , A_1 and h_1^+ , such that the non-standard decay modes are kinematically allowed. From figure 2 it can be observed that the decay branchings depend mildly on the ratio of the mixing angles θ_L and θ_R , once we are away from the narrow peak region. Also the decay branchings of h_2 , A_1 and h_1^+ to tau leptons depend on the yukawa couplings and are almost independent of the masses of the scalars.

Benchmarks	m_{xu_3}	$\text{Br}(xu_3 \rightarrow h_2 t)$	$\text{Br}(xu_3 \rightarrow A_1 t)$	$\text{Br}(xu_3 \rightarrow h_1^+ b)$	$\sigma(pp \rightarrow xu_3, \bar{xu}_3)$
BP1	1 TeV	0.26	0.26	0.48	32.33 fb
BP2	1.5 TeV	0.255	0.255	0.49	1.554 fb
BP3	2 TeV	0.25	0.25	0.5	0.113 fb

TABLE 3: Different benchmark scenarios we have used in collider analysis.

VI. COLLIDER ANALYSIS

Now we consider the collider signatures of xu_3 for 13 TeV LHC in the scenario where the pair produced xu_3 will decay to the final states th_2 , tA_1 , bh_1^+ and the scalars h_2 , A_1 and h_1^+ will further decay to tau leptons. Taking into account all possible decay chains of xu_3 , fig.3 shows all possible final states that can arise from the pair production of xu_3 . Since each final state contains at least two tau leptons and at least one b quark, we choose the final state with at least two τ -tagged jets, at least three non τ -tagged jets among which at least one is b -tagged, and at least one lepton ($\geq 3j(1b) + \geq 2\tau + \geq 1l$) for the collider analysis.

The possible SM processes that can contribute as background to the above choice of final

state are the following:

- $pp \rightarrow t\bar{t} + \text{jets}$,
- $pp \rightarrow t\bar{t} l^+ l^- + \text{jets}$ and $pp \rightarrow t\bar{t} \tau^+ \tau^- + \text{jets}$,
- $pp \rightarrow t\bar{t} l^+ \nu_l + \text{jets}$ and $pp \rightarrow t\bar{t} \tau^+ \nu_\tau + \text{jets}$,
- $pp \rightarrow ZZZ$,
- $pp \rightarrow W^\pm/Z + \text{jets}$.

Among all the above possible backgrounds the most dominant one is $t\bar{t} + \text{jets}$. Although the cross section for the backgrounds $W^\pm/Z + \text{jets}$ is large it is possible to get rid of this by a large E_T requirement which we have used in our analysis. The contribution of ZZZ will be negligible because of its small cross section. Hence we consider only the first three of the above list of backgrounds for the collider analysis in the context of 13 TeV LHC.

To study the collider phenomenology we implemented the model in the spectrum-generator-generator **SARAH** [59]. The source code generated by **SARAH** for the spectrum generator **SPheno** [60] has been used in **SPheno** to study the spectrum of the model. The files generated by **SARAH** in the **UFO** format and the spectrum file generated by **SPheno** has been used in **MadGraph 5** [61] for event generation for the signal. The background events have also been generated using **Madgraph 5**. For showering and hadronization we used **Pythia 6** [62] interfaced in **Madgraph 5**. **DELPHES 3** [63] within CMS environment has been used to take into account the detector effects and also for reconstruction of the final state objects. The anti- k_T algorithm with cone size 0.5 have been used for the jet reconstruction. For the reconstruction of the jets, **FastJet** [64] embedded in **DELPHES** has been used. **MadAnalysis 5** [65] package has been used for the event-analysis using the event format **ROOT** and **LHCO**.

The selection criteria for the final state objects in the reconstructed events are such that a non τ -tagged jet with $p_T(j) > 20$ GeV and $|\eta(j)| < 2.5$ is considered in the event, an electron or a muon with $p_T(l) > 10$ GeV and $|\eta(l)| < 2.5$ are considered in the event, a τ -tagged jet with $p_T(\tau) > 20$ GeV and $|\eta(\tau)| < 2.5$ is considered in the event. Note that here j denotes a non τ -tagged jet, τ denotes a τ -tagged jet. A non τ -tagged jet (j) is either a light jet or a b -tagged jet. The minimum angular separation between all final state objects satisfy $\Delta R > 0.4$. The τ -tagging and mistagging efficiencies are incorporated in **Delphes3** as reported by the ATLAS collaboration [66]. We operate our simulation on the Medium tag point for which the tagging efficiency of 1-prong (3-prong) τ decay is 70% (60%) and the corresponding mistagging rate is 1% (2%).

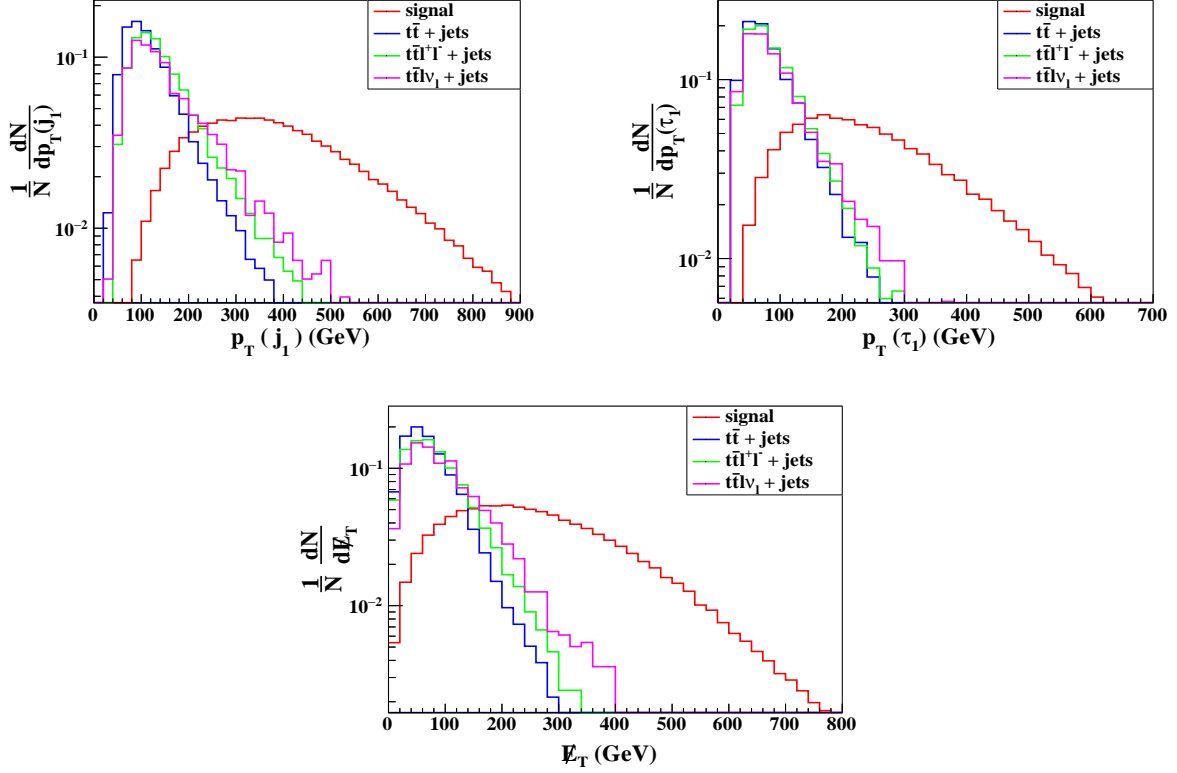


FIG. 4: Normalized distributions for the transverse momentum for the leading non τ -tagged jet ($P_T(j_1)$), the transverse momentum for the leading τ -tagged jet ($P_T(\tau_1)$) and the total missing transverse energy E_T^{miss} for BP1 with $m_{xu_3} = 1$ TeV.

A. BP1 : $m_{xu_3} = 1$ TeV with 100 fb^{-1}

For BP1 the production cross-section and different branching ratios are tabulated in table 3. For the background simulation we generated $pp \rightarrow t\bar{t}$ events up to two additional jets at the leading order accuracy and used *shower- K_T* matching scheme in **Madgraph 5** to avoid the double counting between the partonic events and showered events. For the event analysis we used the cross section for 13 TeV at the NNLO accuracy for top quark pair production, i.e., 815.96 pb[67]. By following the same procedure we have generated both the $t\bar{t}l^+l^-$ and $t\bar{t}l\nu_l$ events up to two additional jets at the leading order accuracy. The obtained leading order cross section at the parton level for $t\bar{t}l^+l^- + \leq 2\text{jets}$ is 96 fb for 13 TeV LHC and to accommodate the NLO effects we multiplied the cross section with a factor of 1.4 which is the NLO K-factor for $t\bar{t}Z$. Similarly for $t\bar{t}l\nu_l + \leq 2\text{jets}$ we multiply the leading order parton level cross section 166 fb for 13 TeV LHC with 1.4 which is the K-factor for $t\bar{t}W$ [61].

After the event selection we compare the phase space behavior of the signal events with

the background and plot the normalized distributions of the transverse momentum (p_T) of the leading non τ -tagged jet and leading τ -tagged jet along with (E_T) in fig. 4. Due to the large mass separation between the VLQ and the scalars, the leading jet is expected to be quite hard as the figure shows. In addition, the τ which comes from the decay of the scalar which is around 300 GeV in mass is also quite hard in p_T . Thus one can make a quite easy separation of the signal and background events using the distributions shown in 4. Based on the distributions and to further optimize the signal-to-background ratio, we apply the following kinematic cuts on the final state objects:

$$p_T(j_1) \geq 200 \text{ GeV}, \quad p_T(\tau_1) \geq 150 \text{ GeV}, \quad E_T \geq 150 \text{ GeV}. \quad (54)$$

With an integrated luminosity of 100 fb^{-1} the cut flow for the signal and background events is shown in table 4a. With the above cuts and with 100 fb^{-1} integrated luminosity, the statistical significance for BP1 is quite large ($\sim 12\sigma$). We have used $\sqrt{2((s+b) \ln(1 + \frac{s}{b}) - s)}$ to calculate the significance. Thus BP1 seems to be have VLQs in a mass range which would be very close to the current sensitivity of the LHC run if such a final state is analyzed for VLQs decaying in non-standard channels as in our model.

B. BP2 : $m_{xu_3} = 1.5 \text{ TeV}$ with 3000 fb^{-1}

For BP2 the branching ratios of xu_3 for the decay modes $h_2 t$, $A_2 t$ and $h_2^+ t$ are around 25.5%, 25.5% and 49% respectively. The background events and their corresponding cross sections are same as in case of BP1 and we have used the same preselection criteria on the events (i.e. $\geq 3j(1b) + \geq 2\tau + \geq 1l$) for BP2. The differences between the mass of the VLQ xu_3 and the masses of scalars (h_2 , A_1 , h_1^+) increase as we go higher in values of the mass of xu_3 while keeping the mass of the scalars fixed as before. It is worth pointing out here that even if the mass of the scalars are made larger, the decay probabilities of the VLQ do not change much. Therefore the event rates would remain the same, albeit the cut efficiencies would change due to new thresholds for the leading jet and tagged τ . Note that the b quark that will originate from the decay $xu_3 \rightarrow h_1^+ b$ for a 1.5 TeV xu_3 will have a large p_T compared to the b quark that originates from the decay of a 1 TeV xu_3 . Since the leading non τ -tagged jet is most likely the b jet coming from $h_1^+ b$ mode it will be in general harder in BP2 compared to BP1. Accordingly for BP2, we have applied the following selection criteria on the final state objects from the reconstructed events to optimize the significance :

$$p_T(j_1) \geq 300 \text{ GeV}, \quad p_T(\tau_1) \geq 200 \text{ GeV}, \quad E_T \geq 200 \text{ GeV}. \quad (55)$$

Notice after the cut on $p_T(j_1)$ to further improve the significance we have also applied cuts with higher values on $p_T(\tau_1)$ and E_T compared to the scenario of BP1. For BP2 with

BP1 : $m_{xu_3} = 1 \text{ TeV}$, $\mathcal{L} = 100 \text{ fb}^{-1}$		
Cuts	No. of Events	
	Signal	Background
Preselection	365	19677
$p_T(j_1) \geq 200 \text{ GeV}$	320	2959
$p_T(\tau_1) \geq 150 \text{ GeV}$	245	839
$E_T \geq 150 \text{ GeV}$	188	191

(a)

BP2 : $m_{xu_3} = 1.5 \text{ TeV}$, $\mathcal{L} = 3000 \text{ fb}^{-1}$		
Cuts	No. of Events	
	Signal	Background
Preselection	455	590310
$p_T(j_1) \geq 300 \text{ GeV}$	401	28547
$p_T(\tau_1) \geq 200 \text{ GeV}$	307	6050
$E_T \geq 200 \text{ GeV}$	245	1455

(b)

BP3 : $m_{xu_3} = 2 \text{ TeV}$, $\mathcal{L} = 3000 \text{ fb}^{-1}$		
Cuts	No. of Events	
	Signal	Background
Preselection	86	856721
$p_T(j_1) \geq 350 \text{ GeV}$	81	269121
$p_T(j_2) \geq 100 \text{ GeV}$	78	252922
$p_T(\tau_1) \geq 150 \text{ GeV}$	58	57285
$E_T \geq 200 \text{ GeV}$	52	11571
$M_{eff} \geq 2.6 \text{ TeV}$	40	378

(c)

TABLE 4: Cut flow table for BP1 with 100 fb^{-1} , BP2 with 3000 fb^{-1} and BP3 with 3000 fb^{-1} luminosity.

3000 fb^{-1} luminosity the cut flow can be found in the table.4b. Using the survived events after the E_T cut we get a significance around 6.2σ for BP2 with the high-luminosity (HL) option at the LHC.

C. BP3 : $m_{xu_3} = 2 \text{ TeV}$ with 3000 fb^{-1}

Finally for the last benchmark, we choose a very heavy mass of 2 TeV for the VLQ. Quite clearly the event rates would suffer from the very small production cross section and if we require two isolated τ -jets then the final events yield becomes extremely low even with an integrated luminosity of 3000 fb^{-1} . To counter the suppression due to small production cross section we modify our signal choice to a more inclusive channel given by : ≥ 3 non τ -tagged jets out of which one is b -tagged, at least one τ -tagged jet and at least one lepton in the final state.

As we go higher in the mass of xu_3 the probability for the jets and the tau leptons for the signal to have higher p_T values is more compared to the backgrounds. Hence for BP3 with $m_{xu_3} = 2$ TeV to get a large statistics for the $t\bar{t} + jets$ background, we have generated $pp \rightarrow t\bar{t} + 2j$ events exclusively at the parton level for 13 TeV LHC with the following criteria :

- For each event at least one top quark decays leptonically, because at the analysis level we have considered events with at least one lepton in the final state.
- All the jets and leptons satisfy $|\eta| < 3.0$ and the angular separation (ΔR) between all pairs of final state particles are greater than 0.4 (except for leptons where they are separated from each other with minimum angular separation 0.2).
- All the final state objects satisfy $p_T > 10$ GeV.
- The two leading jets in p_T satisfy $p_T(j_1) > 250$ GeV and $p_T(j_2) > 100$ GeV.

With the above cuts the parton level cross section at the leading order accuracy for $pp \rightarrow t\bar{t} + 2j$ with 13 TeV LHC is around 6.18 pb. The same events and cross sections as in case of BP1 has been used for the other two backgrounds $t\bar{t}l^+l^- + jets$ and $t\bar{t}l\nu_l + jets$. Note that with much stronger threshold requirements for the final state jets, we expect that the lesser-order processes involving $t\bar{t}$ and $t\bar{t} + 1j$ would not contribute much, where the extra jet comes from the showering. We then follow the usual procedure of using the **Pythia** showering and **DELPHES 3** simulation to generate the final objects from the $pp \rightarrow t\bar{t} + 2j$ process.

For our analysis, we further demand the following set of cuts on our final state events to improve the significance :

$$p_T(j_1) > 350 \text{ GeV}, p_T(j_2) > 100 \text{ GeV}, p_T(\tau_1) > 150 \text{ GeV}, \\ E_T > 200 \text{ GeV}, M_{eff} > 2.6 \text{ TeV}. \quad (56)$$

Here the effective mass variable (M_{eff}) is defined as the scalar sum of all the transverse momenta in an event and is given by

$$M_{eff} = \sum_{j \in jets} p_T(j) + \sum_{l \in leptons} p_T(l) + E_T. \quad (57)$$

The corresponding cut flow can be seen from the table 4c where we have achieved a signal significance of 2σ for BP3.

We plot the significance as a function of luminosity in figure 5 for all the benchmark points. It is evident that for BP1 significance of 5σ can be achieved with 17.3 fb^{-1} of data,

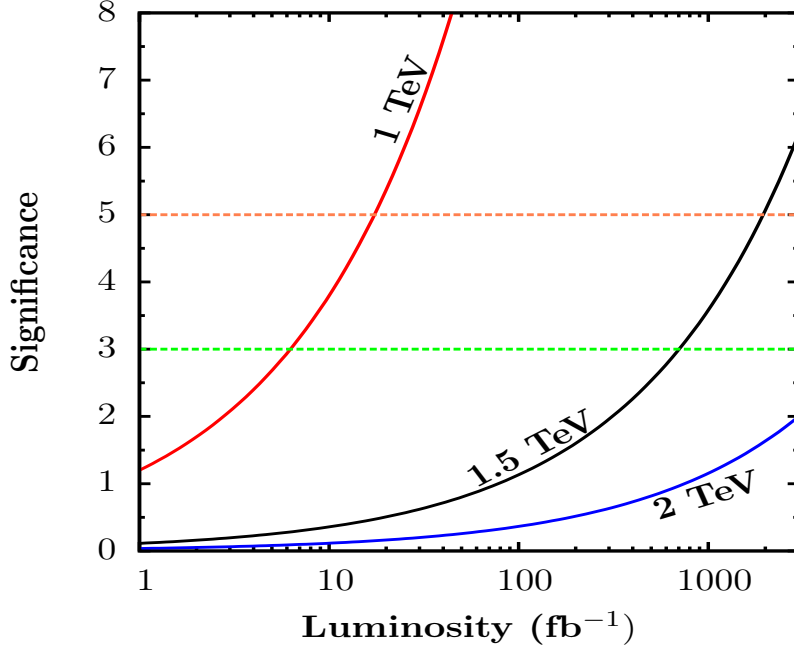


FIG. 5: Significance as a function of luminosity for BP1(1 TeV), BP2(1.5 TeV) and BP3(2 TeV) for 13 TeV LHC.

hence with the already existing datasets of 36.1 fb^{-1} of data would be sensitive to this mass range. With high luminosity data the BP2 can be discovered while it is only possible to exclude a 2 TeV VLQ at 2σ . In fact, an upgrade in LHC energies and higher luminosities would be required to access VLQ signals in such models beyond VLQ mass of $\sim 1.8 \text{ TeV}$. Definitive improvements in the sensitivity is also expected with more sophisticated analysis using boosted studies for the τ states coming from the decay of the heavily boosted scalars.

VII. CONCLUSION

In this work we have considered vector-like quarks in a leptophobic 221 model. Since SM leptons are singlets under the second $SU(2)$, exotic quarks are necessary to cancel triangle anomalies in this model. The exotic quarks become vector-like after the symmetry breaking of the full symmetry group to the SM gauge group. We discussed a particular mixing pattern between SM quarks and VLQs which avoids tree level FCNC interactions. We also find that the same mixing pattern allows for certain neutral scalars to be flavour-conserving in nature. Two of these neutral scalars and their charged partner are tauphilic in nature. These scalars open up non-standard decay modes for the VLQs in the model. We studied the collider signatures for pair production of third generation top-like VLQ when it decays

to final states with any of the tauphilic scalars and a third generation SM quark. Due to the mass hierarchy in the charged lepton sector, these scalars dominantly decay to tau leptons with more than 99% probability. We do an analysis for the signal of such VLQs, pair produced at the LHC with $\sqrt{s} = 13$ TeV through the $\geq 3j(1b) + \geq 2\tau + \geq 1l$ final state, dictated by the decay properties of the VLQ and the new tauphilic scalars. We use mass threshold driven kinematic selections for the final state objects and show the values of the integrated luminosity required for the discovery of such a top-like VLQ for different benchmark points. We find that the amount of data collected till date by the ATLAS and CMS collaborations for 13 TeV LHC is sufficient to confirm or refute the existence of such a scenario for a 1 TeV top-like VLQ. Heavier VLQ masses up to 1.8 TeV would be accessible with the HL option of LHC. This study also highlights an important point of caution for VLQ searches in the standard decay channels carried out at the LHC, that any new physics scenario which may have additional gauge bosons and scalars can alter the VLQ searches in a significant way and therefore alternative channels of search should also be considered, as the VLQ mass limits crucially depend on them [28].

ACKNOWLEDGMENTS

K.D. would like to thank Tianjun Li for useful discussions, Jyotiranjana Beuria for help regarding SARAH and SPheno, Manuel E. Krauss and Subhadeep Mondal for help regarding SARAH. The work was partially supported by funding available from the Department of Atomic Energy, Government of India, for the Regional Centre for Accelerator-based Particle Physics (RECAPP), Harish-Chandra Research Institute. The research of K.D. was supported in part by the INFOSYS scholarship for senior students at the Harish-Chandra Research Institute. The authors acknowledge the use of the High Performance Scientific Computing facility at RECAPP and HRI.

Appendix A: Tadpole equations

The set of tadpole equations $\{\frac{\partial V}{\partial \phi_1^{0r}} = 0, \frac{\partial V}{\partial \phi_2^{0r}} = 0, \frac{\partial V}{\partial \chi^{0r}} = 0, \frac{\partial V}{\partial \chi'^{0r}} = 0\}$ in terms of $\mu_1^2, \mu_2^2, \mu_3^2, \mu_4^2$ are given by

$$\mu_1^2 = \frac{1}{2(v_1^2 - v_2^2)} \{ \alpha_1 u^2 v_1^2 - \alpha_1 u^2 v_2^2 - \alpha_3 u^2 v_2^2 + 2\lambda_1 v_1^4 + 4\lambda_4 v_2 v_1^3 - 4\lambda_4 v_2^3 v_1 - 2\lambda_1 v_2^4 \\ + \sqrt{2} u v_3 (M_1 v_1 - M_2 v_2) + v_3^2 (\beta_1 v_1^2 - (\beta_1 + \beta_3) v_2^2) \}, \quad (\text{A1})$$

$$\mu_2^2 = \frac{1}{4(v_1^2 - v_2^2)} \{ 2\alpha_2 u^2 v_1^2 + \alpha_3 u^2 v_2 v_1 - 2\alpha_2 u^2 v_2^2 + 2\lambda_4 v_1^4 + 8\lambda_2 v_2 v_1^3 + 4\lambda_3 v_2 v_1^3 \\ - 8\lambda_2 v_2^3 v_1 - 4\lambda_3 v_2^3 v_1 - 2\lambda_4 v_2^4 + \sqrt{2} u v_3 (M_2 v_1 - M_1 v_2) \}$$

$$+ v_3^2 (2\beta_2 (v_1^2 - v_2^2) + \beta_3 v_1 v_2) \}, \quad (\text{A2})$$

$$\mu_3^2 = \frac{1}{2v_3} \{ \sqrt{2}u (M_1 v_1 + M_2 v_2) + v_3 (\rho_3 u^2 + \beta_1 v_1^2 + 4\beta_2 v_1 v_2 + (\beta_1 + \beta_3) v_2^2) + 2\rho_1 v_3^3 \}, \quad (\text{A3})$$

$$\mu_4^2 = \frac{1}{2u} \{ v_1 (\sqrt{2}M_1 v_3 + 4\alpha_2 u v_2) + \sqrt{2}M_2 v_2 v_3 + u (2\rho_2 u^2 + (\alpha_1 + \alpha_3) v_2^2 + \rho_3 v_3^2) + \alpha_1 u v_1^2 \}. \quad (\text{A4})$$

Appendix B: Mass matrices for the scalar Sector

1. CP even scalars

The components of the CP even scalar sector mass square matrix(M_S^2) in the $(\phi_1^{0r}, \phi_2^{0r}, \chi'^{0r}, \chi^{0r})$ basis is given by

$$\begin{aligned} (M_S^2)_{11} &= \frac{1}{2(v_1^2 - v_2^2)} \{ v_2 (\sqrt{2}M_2 u v_3 + \alpha_3 u^2 v_2 - 4(2\lambda_2 + \lambda_3) v_2^3) - v_1 (\sqrt{2}M_1 u v_3 + 8\lambda_4 v_3^3) \\ &\quad + \beta_3 v_2^2 v_3^2 + 4\lambda_1 v_1^4 + 8\lambda_4 v_2 v_1^3 + 4(-\lambda_1 + 2\lambda_2 + \lambda_3) v_2^2 v_1^2 \} \\ (M_S^2)_{12} &= \frac{1}{2(v_1^2 - v_2^2)} \{ -v_1 (\sqrt{2}M_2 u v_3 + \alpha_3 u^2 v_2 + 4(\lambda_1 + 2\lambda_2 + \lambda_3) v_2^3) + \sqrt{2}M_1 u v_2 v_3 \\ &\quad - \beta_3 v_2 v_3^2 v_1 + 4\lambda_4 v_1^4 + 4(\lambda_1 + 2\lambda_2 + \lambda_3) v_2 v_1^3 - 4\lambda_4 v_2^4 \} \\ (M_S^2)_{13} &= \frac{M_1 v_3}{\sqrt{2}} + u(\alpha_1 v_1 + 2\alpha_2 v_2) \\ (M_S^2)_{14} &= \frac{M_1 u}{\sqrt{2}} + v_3(\beta_1 v_1 + 2\beta_2 v_2) \\ (M_S^2)_{22} &= \frac{1}{2(v_1^2 - v_2^2)} \{ -v_1 (\sqrt{2}M_1 u v_3 + 8\lambda_4 v_2^3) + \sqrt{2}M_2 u v_2 v_3 + \beta_3 v_3^2 v_1^2 + 4(2\lambda_2 + \lambda_3) v_1^4 \\ &\quad + 8\lambda_4 v_2 v_1^3 - 4\lambda_1 v_2^4 + v_1^2 (\alpha_3 u^2 + 4(\lambda_1 - 2\lambda_2 - \lambda_3) v_2^2) \} \\ (M_S^2)_{23} &= \frac{M_2 v_3}{\sqrt{2}} + u(2\alpha_2 v_1 + (\alpha_1 + \alpha_3) v_2) \\ (M_S^2)_{24} &= \frac{M_2 u}{\sqrt{2}} + v_3(2\beta_2 v_1 + (\beta_1 + \beta_3) v_2) \\ (M_S^2)_{33} &= \frac{1}{2u} \{ 4\rho_2 u^3 - \sqrt{2}v_3 (M_1 v_1 + M_2 v_2) \} \\ (M_S^2)_{34} &= \frac{M_1 v_1}{\sqrt{2}} + \frac{M_2 v_2}{\sqrt{2}} + \rho_3 u v_3 \\ (M_S^2)_{44} &= \frac{1}{2v_3} \{ 4\rho_1 v_3^3 - \sqrt{2}u (M_1 v_1 + M_2 v_2) \} \end{aligned} \quad (\text{B1})$$

2. CP odd scalars

The components of the CP odd scalar sector mass square matrix(M_P^2) in the $(\phi_1^{0i}, \phi_2^{0i}, \chi'^{0i}, \chi^{0i})$ basis is given by

$$\begin{aligned}
(M_P^2)_{11} &= \frac{1}{2(v_1^2 - v_2^2)} \{ \sqrt{2}uv_3(M_2v_2 - M_1v_1) + v_2^2(\alpha_3u^2 - 4(2\lambda_2 - \lambda_3)(v_1^2 - v_2^2)) + \beta_3v_3^2v_2^2 \} \\
(M_P^2)_{12} &= \frac{1}{2(v_1^2 - v_2^2)} \{ \sqrt{2}uv_3(M_2v_1 - M_1v_2) + v_1v_2(\alpha_3u^2 - 4(2\lambda_2 - \lambda_3)(v_1^2 - v_2^2)) + \beta_3v_1v_2v_3^2 \} \\
(M_P^2)_{13} &= -\frac{M_1v_3}{\sqrt{2}} \\
(M_P^2)_{14} &= \frac{M_1u}{\sqrt{2}} \\
(M_P^2)_{22} &= \frac{1}{2(v_1^2 - v_2^2)} \{ \sqrt{2}uv_3(M_2v_2 - M_1v_1) + v_1^2(\alpha_3u^2 - 4(2\lambda_2 - \lambda_3)(v_1^2 - v_2^2)) + \beta_3v_3^2v_1^2 \} \\
(M_P^2)_{23} &= \frac{M_2v_3}{\sqrt{2}} \\
(M_P^2)_{24} &= -\frac{M_2u}{\sqrt{2}} \\
(M_P^2)_{33} &= -\frac{v_3(M_1v_1 + M_2v_2)}{\sqrt{2}u} \\
(M_P^2)_{34} &= \frac{M_1v_1 + M_2v_2}{\sqrt{2}} \\
(M_P^2)_{44} &= -\frac{u(M_1v_1 + M_2v_2)}{\sqrt{2}v_3}
\end{aligned} \tag{B2}$$

3. Charged scalars

The mass square matrix for the charged scalars (M_C^2) in the $(\phi_1^+, \phi_2^+, \chi'^+, \chi^+)$ basis is given by

$$\begin{aligned}
(M_C^2)_{11} &= \frac{1}{2(v_1^2 - v_2^2)} \{ u(\sqrt{2}v_3(M_2v_2 - M_1v_1) + \alpha_3uv_2^2) + \beta_3v_1^2v_3^2 \} \\
(M_C^2)_{12} &= \frac{1}{2(v_1^2 - v_2^2)} \{ u(\sqrt{2}v_3(M_2v_1 - M_1v_2) + \alpha_3uv_1v_2) + \beta_3v_1v_2v_3^2 \} \\
(M_C^2)_{13} &= -\frac{M_2v_3}{\sqrt{2}} - \frac{1}{2}\alpha_3uv_2 \\
(M_C^2)_{14} &= \frac{M_1u}{\sqrt{2}} - \frac{1}{2}\beta_3v_1v_3 \\
(M_C^2)_{22} &= \frac{1}{2(v_1^2 - v_2^2)} \{ u(\sqrt{2}v_3(M_2v_2 - M_1v_1) + \alpha_3uv_1^2) + \beta_3v_2^2v_3^2 \} \\
(M_C^2)_{23} &= \frac{M_1v_3}{\sqrt{2}} - \frac{1}{2}\alpha_3uv_1
\end{aligned}$$

$$\begin{aligned}
(M_C^2)_{24} &= -\frac{M_2 u}{\sqrt{2}} - \frac{1}{2}\beta_3 v_2 v_3 \\
(M_C^2)_{33} &= \frac{1}{2} \left(\alpha_3 (v_1^2 - v_2^2) - \frac{\sqrt{2} v_3 (M_1 v_1 + M_2 v_2)}{u} \right) \\
(M_C^2)_{34} &= \frac{M_2 v_1 + M_1 v_2}{\sqrt{2}} \\
(M_C^2)_{44} &= \frac{1}{2v_3} \{ \beta_3 (v_1^2 - v_2^2) v_3 - \sqrt{2} u (M_1 v_1 + M_2 v_2) \}
\end{aligned} \tag{B3}$$

-
- [1] O. Eberhardt, G. Herbert, H. Lacker, A. Lenz, A. Menzel, U. Nierste et al., *Impact of a Higgs boson at a mass of 126 GeV on the standard model with three and four fermion generations*, *Phys. Rev. Lett.* **109** (2012) 241802 [1209.1101].
 - [2] CMS collaboration, A. M. Sirunyan et al., *Search for vector-like T and B quark pairs in final states with leptons at $\sqrt{s} = 13$ TeV*, 1805.04758.
 - [3] CMS collaboration, A. M. Sirunyan et al., *Search for pair production of vector-like quarks in the $bW\bar{b}W$ channel from proton-proton collisions at $\sqrt{s} = 13$ TeV*, *Phys. Lett.* **B779** (2018) 82 [1710.01539].
 - [4] ATLAS collaboration, M. Aaboud et al., *Search for pair- and single-production of vector-like quarks in final states with at least one Z boson decaying into a pair of electrons or muons in pp collision data collected with the ATLAS detector at $\sqrt{s} = 13$ TeV*, 1806.10555.
 - [5] ATLAS collaboration, M. Aaboud et al., *Search for pair production of heavy vector-like quarks decaying into high- p_T W bosons and top quarks in the lepton-plus-jets final state in pp collisions at $\sqrt{s} = 13$ TeV with the ATLAS detector*, 1806.01762.
 - [6] ATLAS collaboration, M. Aaboud et al., *Search for pair production of up-type vector-like quarks and for four-top-quark events in final states with multiple b -jets with the ATLAS detector*, 1803.09678.
 - [7] ATLAS collaboration, M. Aaboud et al., *Search for pair production of heavy vector-like quarks decaying to high- p_T W bosons and b quarks in the lepton-plus-jets final state in pp collisions at $\sqrt{s} = 13$ TeV with the ATLAS detector*, *JHEP* **10** (2017) 141 [1707.03347].
 - [8] CMS collaboration, A. M. Sirunyan et al., *Search for single production of vector-like quarks decaying to a b quark and a Higgs boson*, *JHEP* **06** (2018) 031 [1802.01486].
 - [9] CMS collaboration, A. M. Sirunyan et al., *Search for single production of a vector-like T quark decaying to a Z boson and a top quark in proton-proton collisions at $\sqrt{s} = 13$ TeV*, *Phys. Lett.* **B781** (2018) 574 [1708.01062].

- [10] *Search for single production of vector-like quarks decaying into Wb in pp collisions at $\sqrt{s} = 13$ TeV with the ATLAS detector*, The ATLAS Collaboration, Report No. ATLAS-CONF-2016-072, 2016 .
- [11] J. A. Aguilar-Saavedra, *Pair production of heavy $Q = 2/3$ singlets at LHC*, *Phys. Lett.* **B625** (2005) 234 [[hep-ph/0506187](#)].
- [12] J. A. Aguilar-Saavedra, *Identifying top partners at LHC*, *JHEP* **11** (2009) 030 [[0907.3155](#)].
- [13] G. Cacciapaglia, A. Deandrea, D. Harada and Y. Okada, *Bounds and Decays of New Heavy Vector-like Top Partners*, *JHEP* **11** (2010) 159 [[1007.2933](#)].
- [14] Y. Okada and L. Panizzi, *LHC signatures of vector-like quarks*, *Adv. High Energy Phys.* **2013** (2013) 364936 [[1207.5607](#)].
- [15] A. De Simone, O. Matsedonskyi, R. Rattazzi and A. Wulzer, *A First Top Partner Hunter's Guide*, *JHEP* **04** (2013) 004 [[1211.5663](#)].
- [16] J. A. Aguilar-Saavedra, R. Benbrik, S. Heinemeyer and M. Pérez-Victoria, *Handbook of vectorlike quarks: Mixing and single production*, *Phys. Rev.* **D88** (2013) 094010 [[1306.0572](#)].
- [17] S. A. R. Ellis, R. M. Godbole, S. Gopalakrishna and J. D. Wells, *Survey of vector-like fermion extensions of the Standard Model and their phenomenological implications*, *JHEP* **09** (2014) 130 [[1404.4398](#)].
- [18] K. Hsieh, K. Schmitz, J.-H. Yu and C. P. Yuan, *Global Analysis of General $SU(2) \times SU(2) \times U(1)$ Models with Precision Data*, *Phys. Rev.* **D82** (2010) 035011 [[1003.3482](#)].
- [19] K. Das, T. Li, S. Nandi and S. K. Rai, *Diboson excesses in an anomaly free leptophobic left-right model*, *Phys. Rev.* **D93** (2016) 016006 [[1512.00190](#)].
- [20] P. Langacker, *The Physics of Heavy Z' Gauge Bosons*, *Rev. Mod. Phys.* **81** (2009) 1199 [[0801.1345](#)].
- [21] J. Kearney, A. Pierce and J. Thaler, *Top Partner Probes of Extended Higgs Sectors*, *JHEP* **08** (2013) 130 [[1304.4233](#)].
- [22] J. Kearney, A. Pierce and J. Thaler, *Exotic Top Partners and Little Higgs*, *JHEP* **10** (2013) 230 [[1306.4314](#)].
- [23] D. Karabacak, S. Nandi and S. K. Rai, *New signal for singlet Higgs and vector-like quarks at the LHC*, *Phys. Lett.* **B737** (2014) 341 [[1405.0476](#)].
- [24] J. Serra, *Beyond the Minimal Top Partner Decay*, *JHEP* **09** (2015) 176 [[1506.05110](#)].
- [25] A. Anandakrishnan, J. H. Collins, M. Farina, E. Kuflik and M. Perelstein, *Odd Top Partners at the LHC*, *Phys. Rev.* **D93** (2016) 075009 [[1506.05130](#)].
- [26] S. Banerjee, D. Barducci, G. Bélanger and C. Delaunay, *Implications of a High-Mass Diphoton Resonance for Heavy Quark Searches*, *JHEP* **11** (2016) 154 [[1606.09013](#)].

- [27] A. Arhrib, R. Benbrik, S. King, B. Manaut, S. Moretti and C. Un, *Phenomenology of 2HDM with vectorlike quarks*, *Phys. Rev.* **D97** (2018) 095015 [1607.08517].
- [28] B. A. Dobrescu and F. Yu, *Exotic Signals of Vectorlike Quarks*, *J. Phys.* **G45** (2016) 08 [1612.01909].
- [29] J. A. Aguilar-Saavedra, D. E. López-Fogliani and C. Muñoz, *Novel signatures for vector-like quarks*, *JHEP* **06** (2017) 095 [1705.02526].
- [30] M. Chala, *Direct bounds on heavy toplike quarks with standard and exotic decays*, *Phys. Rev.* **D96** (2017) 015028 [1705.03013].
- [31] S. Moretti, D. O’Brien, L. Panizzi and H. Prager, *Production of extra quarks decaying to Dark Matter beyond the Narrow Width Approximation at the LHC*, *Phys. Rev.* **D96** (2017) 035033 [1705.07675].
- [32] M. Chala, R. Gröber and M. Spannowsky, *Searches for vector-like quarks at future colliders and implications for composite Higgs models with dark matter*, *JHEP* **03** (2018) 040 [1801.06537].
- [33] N. Bizot, G. Cacciapaglia and T. Flacke, *Common exotic decays of top partners*, *JHEP* **06** (2018) 065 [1803.00021].
- [34] J. H. Kim and I. M. Lewis, *Loop Induced Single Top Partner Production and Decay at the LHC*, *JHEP* **05** (2018) 095 [1803.06351].
- [35] B. N. Grossmann, B. McElrath, S. Nandi and S. K. Rai, *Hidden Extra $U(1)$ at the Electroweak/TeV Scale*, *Phys. Rev.* **D82** (2010) 055021 [1006.5019].
- [36] A. Joglekar and J. L. Rosner, *Searching for signatures of E_6* , *Phys. Rev.* **D96** (2017) 015026 [1607.06900].
- [37] K. Das, T. Li, S. Nandi and S. K. Rai, *New signals for vector-like down-type quark in $U(1)$ of E_6* , *Eur. Phys. J.* **C78** (2018) 35 [1708.00328].
- [38] J. A. Aguilar-Saavedra, *Effects of mixing with quark singlets*, *Phys. Rev.* **D67** (2003) 035003 [hep-ph/0210112].
- [39] G. Cacciapaglia, A. Deandrea, L. Panizzi, N. Gaur, D. Harada and Y. Okada, *Heavy Vector-like Top Partners at the LHC and flavour constraints*, *JHEP* **03** (2012) 070 [1108.6329].
- [40] J. A. Aguilar-Saavedra, *Mixing with vector-like quarks: constraints and expectations*, *EPJ Web Conf.* **60** (2013) 16012 [1306.4432].
- [41] A. K. Alok, S. Banerjee, D. Kumar and S. Uma Sankar, *Flavor signatures of isosinglet vector-like down quark model*, *Nucl. Phys.* **B906** (2016) 321 [1402.1023].
- [42] A. K. Alok, S. Banerjee, D. Kumar, S. U. Sankar and D. London, *New-physics signals of a model with a vector-singlet up-type quark*, *Phys. Rev.* **D92** (2015) 013002 [1504.00517].

- [43] C.-Y. Chen, S. Dawson and E. Furlan, *Vectorlike fermions and Higgs effective field theory revisited*, *Phys. Rev.* **D96** (2017) 015006 [1703.06134].
- [44] P. Langacker and D. London, *Mixing Between Ordinary and Exotic Fermions*, *Phys. Rev.* **D38** (1988) 886.
- [45] R. N. Mohapatra and J. C. Pati, *A Natural Left-Right Symmetry*, *Phys. Rev.* **D11** (1975) 2558.
- [46] R. N. Mohapatra and J. C. Pati, *Left-Right Gauge Symmetry and an Isoconjugate Model of CP Violation*, *Phys. Rev.* **D11** (1975) 566.
- [47] G. Senjanovic and R. N. Mohapatra, *Exact Left-Right Symmetry and Spontaneous Violation of Parity*, *Phys. Rev.* **D12** (1975) 1502.
- [48] G. Senjanovic, *Spontaneous Breakdown of Parity in a Class of Gauge Theories*, *Nucl. Phys.* **B153** (1979) 334.
- [49] R. N. Mohapatra and G. Senjanovic, *Neutrino Mass and Spontaneous Parity Violation*, *Phys. Rev. Lett.* **44** (1980) 912.
- [50] R. N. Mohapatra and G. Senjanovic, *Neutrino Masses and Mixings in Gauge Models with Spontaneous Parity Violation*, *Phys. Rev.* **D23** (1981) 165.
- [51] ATLAS collaboration, G. Aad et al., *Search for high-mass diboson resonances with boson-tagged jets in proton-proton collisions at $\sqrt{s} = 8$ TeV with the ATLAS detector*, *JHEP* **12** (2015) 055 [1506.00962].
- [52] N. G. Deshpande, J. F. Gunion, B. Kayser and F. I. Olness, *Left-right symmetric electroweak models with triplet Higgs*, *Phys. Rev.* **D44** (1991) 837.
- [53] J. F. Gunion, J. Grifols, A. Mendez, B. Kayser and F. I. Olness, *Higgs Bosons in Left-Right Symmetric Models*, *Phys. Rev.* **D40** (1989) 1546.
- [54] ATLAS collaboration, M. Aaboud et al., *Search for new phenomena in dijet events using 37 fb^{-1} of pp collision data collected at $\sqrt{s} = 13$ TeV with the ATLAS detector*, *Phys. Rev.* **D96** (2017) 052004 [1703.09127].
- [55] ATLAS collaboration, M. Aaboud et al., *Search for new high-mass phenomena in the dilepton final state using 36 fb^{-1} of proton-proton collision data at $\sqrt{s} = 13$ TeV with the ATLAS detector*, *JHEP* **10** (2017) 182 [1707.02424].
- [56] J. Erler, P. Langacker, S. Munir and E. Rojas, *Improved Constraints on Z-prime Bosons from Electroweak Precision Data*, *JHEP* **08** (2009) 017 [0906.2435].
- [57] NNPDF collaboration, R. D. Ball et al., *Parton distributions for the LHC Run II*, *JHEP* **04** (2015) 040 [1410.8849].
- [58] DELPHI collaboration, J. Abdallah et al., *Searches for neutral higgs bosons in extended models*, *Eur. Phys. J.* **C38** (2004) 1 [hep-ex/0410017].

- [59] F. Staub, *SARAH 4 : A tool for (not only SUSY) model builders*, *Comput. Phys. Commun.* **185** (2014) 1773 [1309.7223].
- [60] W. Porod and F. Staub, *SPheno 3.1: Extensions including flavour, CP-phases and models beyond the MSSM*, *Comput. Phys. Commun.* **183** (2012) 2458 [1104.1573].
- [61] J. Alwall, R. Frederix, S. Frixione, V. Hirschi, F. Maltoni, O. Mattelaer et al., *The automated computation of tree-level and next-to-leading order differential cross sections, and their matching to parton shower simulations*, *JHEP* **07** (2014) 079 [1405.0301].
- [62] T. Sjostrand, S. Mrenna and P. Z. Skands, *PYTHIA 6.4 Physics and Manual*, *JHEP* **05** (2006) 026 [hep-ph/0603175].
- [63] DELPHES 3 collaboration, J. de Favereau, C. Delaere, P. Demin, A. Giammanco, V. Lemaître, A. Mertens et al., *DELPHES 3, A modular framework for fast simulation of a generic collider experiment*, *JHEP* **02** (2014) 057 [1307.6346].
- [64] M. Cacciari, G. P. Salam and G. Soyez, *FastJet User Manual*, *Eur. Phys. J. C* **72** (2012) 1896 [1111.6097].
- [65] E. Conte, B. Fuks and G. Serret, *MadAnalysis 5, A User-Friendly Framework for Collider Phenomenology*, *Comput. Phys. Commun.* **184** (2013) 222 [1206.1599].
- [66] ATLAS collaboration, *Reconstruction, Energy Calibration, and Identification of Hadronically Decaying Tau Leptons in the ATLAS Experiment for Run-2 of the LHC*, Report No. *ATL-PHYS-PUB-2015-045* (2015) .
- [67] M. Czakon and A. Mitov, *Top++: A Program for the Calculation of the Top-Pair Cross-Section at Hadron Colliders*, *Comput. Phys. Commun.* **185** (2014) 2930 [1112.5675].